



The nitrogen budget of laboratory-simulated western U.S. wildfires during the FIREX 2016 FireLab study

James M. Roberts¹, Chelsea E. Stockwell^{1,2@}, Robert J. Yokelson³, Joost de Gouw^{1,2,5}, Yong Liu⁴, Vanessa Selimovic³, Abigail R. Koss^{1,2,5*}, Kanako Sekimoto^{1,2,6}, Matthew M. Coggon^{1,2}, Bin Yuan^{1,2,†}, Kyle J. Zarzana^{1,2,Δ}, Steven S. Brown¹, Cristina Santin⁷, Stefan H. Doerr⁷, and Carsten Warneke^{1,2}

¹NOAA Earth System Research Laboratories (ESRL), Chemical Sciences Laboratory, Boulder, CO, USA.

²Cooperative Institute for Research in Environmental Sciences, University of Colorado Boulder, Boulder, CO, USA.

³Department of Chemistry and Biochemistry, University of Montana, Missoula, MT, USA.

⁴Department of Chemistry, University of Colorado, Denver, Denver, Colorado, USA.

⁵Department of Chemistry, University of Colorado Boulder, Boulder, CO, USA.

⁶Graduate School of Nanobioscience, Yokohama City University, Yokohama, Japan.

⁷Department of Geography, Swansea University, Swansea, UK.

* now at Tofwerk, USA, Boulder, CO, USA.

† now at Institute for Environmental and Climate Research, Jinan University, Guangzhou, China.

@ now at Scientific Aviation, Boulder, CO., USA.

Δ now at Department of Chemistry, University of Colorado Boulder, Boulder, CO, USA.

Correspondence to: James M. Roberts (james.m.roberts@noaa.gov)

Abstract. Total reactive nitrogen (N_r , defined as all nitrogen-containing compounds except for N_2 and N_2O) was measured by catalytic conversion to NO and detection by NO- O_3 chemiluminescence together with individual N_r species during a series of laboratory fires of fuels characteristic of Western U.S. wildfires, conducted as part of the FIREX FireLab 2016 study. Data from 75 stack fires were analyzed to examine the systematics of nitrogen emissions. The N_r /total-carbon ratios measured in the emissions were compared with fuel and ash N/C ratios and mass to estimate that a mean (\pm std. dev.) of 0.68 (\pm 0.14) of fuel nitrogen was emitted as N_2 and N_2O . The remaining fraction of N_r was emitted as individual compounds: nitric oxide (NO), nitrogen dioxide (NO_2), nitrous acid (HONO), isocyanic acid (HNCO), hydrogen cyanide (HCN), ammonia (NH_3), and 44 nitrogen-containing volatile organic compounds (NVOCs). The relative difference between the total reactive nitrogen measurement, N_r , and the sum of measured individual N_r compounds had a mean (\pm std. dev.) of 0.152 (\pm 0.098). Much of this “unaccounted” N_r is expected to be particle-bound species, not included in this analysis.

A number of key species, e.g. HNCO, HCN and HONO, were confirmed not to correlate only with flaming or only with smoldering combustion when using modified combustion efficiency ($MCE = CO_2/(CO + CO_2)$) as a rough indicator. However, the systematic variations of the abundance of these species relative to other nitrogen-containing species were successfully modeled using positive matrix factorization (PMF). Three distinct factors were found for the emissions from combined coniferous fuels, aligning with our understanding of combustion chemistry in different temperature ranges: a combustion factor (Comb-N) (800-1200°C) with emissions of the inorganic compounds NO, NO_2 and HONO, and a minor contribution from organic nitro compounds (R- NO_2); a high-temperature pyrolysis factor (HT-N) (500-800°C) with emissions of HNCO, HCN and nitriles; and a low-temperature pyrolysis factor (LT-N) (<500°C) with mostly ammonia, and NVOCs, with the temperature ranges being based on known combustion and pyrolysis chemistry considerations. The mix of emissions in the PMF factors from the



chaparral fuels had a slightly different composition: the Comb-N factor was also mostly NO, with small amounts of HNCO, HONO and NH₃, the HT-N factor was dominated by NO₂ and had HONO, HCN, and HNCO, and the LT-N factor was mostly NH₃ with a slight amount of NO contributing. In both cases, the Comb-N factor correlated best with CO₂ emission, while the HT-N factors from coniferous fuels correlated closely with the high temperature VOC factors recently reported by Sekimoto et al., (2018) and the LT-N had some correspondence to the LT-VOC factors. As a consequence, CO₂ is recommended as a marker for combustion N_r emissions, HCN is recommended as a marker for HT-N emissions and the family NH₃/particle ammonium is recommended as a marker for LT-N emissions.

1 Introduction

Wildfires have severe impacts on the chemistry of the atmosphere from local to global scales (Crutzen and Andreae, 1990). A warmer, drier climate in western North America, coupled with policies that have allowed build-up of fuels in forest ecosystems has led to increases in frequency and severity of wildfires in this region (Abatzoglou and Williams, 2016; Westerling et al., 2006). The new strategy for management of wildfire in the U.S. is to allow fire where possible and to fight fire where needed (Lee et al., 2014). The science behind making these decisions and understanding their consequences involves, in part, a better understanding of the emissions from wildfires. The NOAA FIREX (Fire Influence on Regional and Global Environments Experiment) FireLab experiment was conducted in the Fall of 2016, at the U.S. Forest Service Fire Sciences Laboratory in Missoula, Montana, to acquire detailed measurements of particle and gas-phase emissions from fires involving fuels characteristic of the western U.S. (NOAA, 2018). Several aspects of these measurements dealing with VOC species, and individual reactive nitrogen species (N_r, defined as all nitrogen compounds except for N₂ and N₂O) have already been published (Koss et al., 2018; Manfred et al., 2018; Sekimoto et al., 2018; Selimovic et al., 2018; Zarzana et al., 2018), including emissions factors for many of the N_r-species (Koss et al., 2018).

The N_r compounds emitted by natural-convection biomass burning (BB) arise solely from the N in the fuels, since the combustion temperatures are not high enough (<1200°C) to produce NO_x from N₂ and O₂ (the so-called Zeldovich or thermal nitrogen cycle) (Lobert and Warnatz, 1993; Taylor et al., 2004; Wotton et al., 2012). The fuel nitrogen cycles that pertain to BB flaming combustion are shown schematically in Figure 1 (Glarborg et al., 2018; Lobert and Warnatz, 1993; Lucassen et al., 2012). N_r compounds are emitted as small molecules, HCN, HNCO and NH₃ resulting from pyrolysis of the fuel, with minor contributions from larger N-containing organic species, especially at lower temperatures. Flame chemistry converts those species to N₂, N₂O, NO, NO₂, and HONO as a result of radical chemistry. It has been recognized for some time that a significant amount of denitrification (conversion of N_r compounds to N₂) occurs due to reactions of NO with NH_i (where i= 1, 2, or 3) or N atoms, as confirmed experimentally (Kuhlbusch et al., 1991). While N atoms are also intermediates in the thermal NO_x cycle and the reaction N + O₂ => NO + O figures in to both the fuel and thermal NO_x cycles, the second reaction of the thermal NO_x cycle, O + N₂ = NO + N, is too slow at BB flame temperatures to result in NO_x production (Manion et al., 2015). In addition to the small molecules shown in Figure 1, numerous N_r-compounds are emitted in roughly the following categories: amides, amines, heterocyclic compounds, nitriles, isocyanates, and nitro compounds (Andreae, 2019; Andreae and Merlet, 2001; Koss et al., 2018; Lobert et al., 1991; Lobert et al., 1990; Lobert and Warnatz, 1993;



81 Stockwell et al., 2015). These compounds are produced at much lower abundance from fuel pyrolysis and partial
82 reactions with the radical species in Figure 1.

83 The emissions of N-compounds from BB and wildfires in general have been the subject of considerable
84 research (Akagi et al., 2011; Andreae, 2019; Andreae and Merlet, 2001; Burling et al., 2010; Coggon et al., 2016;
85 Gilman et al., 2015; Kuhlbusch et al., 1991; Lobert et al., 1991; Lobert et al., 1990; Lobert and Warnatz, 1993;
86 McMeeking et al., 2009; Stockwell et al., 2015; Veres et al., 2010; Warneke et al., 2011; Yokelson et al., 2013b;
87 Yokelson et al., 2009). The known N-compounds range in oxidation state from NH_3 to HNO_3 and include N_2 and N_2O .
88 Among the more prominent and important N_r species are: NO_x (NO and NO_2) which is a key player in the atmospheric
89 oxidant cycle; NH_3 which has a major role in particle formation; nitrous acid (HONO) which can be an important
90 radical source; hydrogen cyanide and acetonitrile (HCN , CH_3CN) which are toxic at high concentrations and represent
91 valuable tracers for following fire transport; and isocyanates, isocyanic acid and methyl isocyanate (HNCO , CH_3NCO)
92 which have unique health impacts (Roberts et al., 2011). In addition, nitro ($-\text{NO}_2$), or nitrogen heterocyclic compounds
93 may contribute to so-called brown carbon, aerosol organic compounds exhibiting optical absorption in the near-UV
94 or blue wavelength regions. Wildfire N emissions also have very minor contributions from gas phase nitric acid
95 (HNO_3). Nitric acid is either not efficiently produced by BB or is readily incorporated into aerosol if it is produced in
96 fresh wildfire plumes, as is clear from the absence of HNO_3 enhancements in several studies of BB plumes (Liu et al.,
97 2016; Yokelson et al., 2009) (Alvarado et al., 2010), however nitrate (NO_3^-) has been shown to contribute to aerosol
98 mass particularly for inefficient combustion (May et al., 2014). Flame chemistry is inefficient in forming N_2O , relative
99 to the pathways that form N_2 (Andreae, 2019; Andreae and Merlet, 2001; Griffith et al., 1991; Hao et al., 1991). The
100 modeling of the emissions of these N-compounds on a large scale could benefit from a better understanding of the
101 total budget of these species as a function of fuel nitrogen content and the dependence of the individual species on
102 fuel type and combustion conditions.

103 The construction of N_r -budgets in this work is made possible by the inclusion of a total reactive nitrogen
104 measurement (termed N_r herein), a method by which all nitrogen compounds besides N_2 and N_2O are converted to NO
105 and detected by NO-O_3 chemiluminescence. This technology has been developed by a number of groups, typically
106 using precious metal or NiCr catalysts that have been shown to convert all N_r compounds to NO (and to some extent
107 NO_2) at high temperatures ($750\text{--}825^\circ\text{C}$) (Hardy and Knarr, 1982; Kashihiro et al., 1982; Marx et al., 2012; Roberts et
108 al., 1988). There are also commercial instruments that incorporate this technology (see for example Thermo Scientific
109 Model 17i). This technique has been applied to gas phase atmospheric measurements, principally to measure NH_3 by
110 difference techniques (Saylor et al., 2010; Schwab et al., 2007), and has also been used to observe wildfire plumes
111 that have impacted ambient air measurements (Benedict et al., 2017; Prenni et al., 2014). We have recently developed
112 a platinum/molybdenum oxide N_r catalyst system, and confirmed that it quantitatively converts N_r compounds
113 including all particle-bound nitrogen compounds (Stockwell et al., 2018). To our knowledge this technique has not
114 been applied directly to BB emissions before.

115 This paper will describe the total reactive nitrogen, and individual N_r compound measurements made during
116 the FireLab 2016 experiment. The total N_r measurements will be combined with CO_2 , CO , and VOC measurements
117 and fuel, residue and ash C and N content to estimate the amount of N lost to N_2 and N_2O . Fire-integrated N_r will be



compared to fire-integrated measurements of individual compounds to determine the fraction of unaccounted-for N_r . The systematic behavior of individual N_r species and their fractional contribution to N_r will be examined with respect to fuel type, N content, and combustion processes. A positive matrix factorization (PMF) technique will be used to examine commonalities between fires of different fuels under different conditions and compared to the PMF analysis of the VOC emissions published by Sekimoto et al., (2018). The results will be used to arrive at suggested guidelines that can be used estimate N_r -emissions profiles for fires representative of western North America.

2 Methodology

The FireLab 2016 study involved laboratory burns of fuels mostly characteristic of western North American wildfires, but also some that have global significance such as Indonesian peat and yak dung. The procedures and associated details of the study have been described previously by Selimovic et al., (2018) and will be only briefly summarized here. The detailed data on fuel types, amounts and composition can be found in Table S1, and in the Supplemental section of Selimovic, et al., (2018). The laboratory burns involved fuel samples, ranging in mass from 0.26 to 6.02 kg. Fires were started without the addition of any contaminants, using an electric igniter (a series of NiCr heating elements that were flash-heated electrically), and typically lasted from approximately 5 to 30 minutes. Seventy-five fires were conducted in the configuration where the smoke was directed up the central stack of the facility where it could be sampled simultaneously by all the instruments that measured gas phase species, and some of the particle phase measurements. The sampling platform was about 15 m above the fire and the sampling took place in well-mixed smoke approximately 5s after emission (Christian et al., 2004). Thirty-one additional fires were conducted on most of the same fuels, when the stack was closed and the room was allowed to fill with smoke, permitting sampling to be done over the course of several hours. The following analyses will focus on the “stack” burns, as those measurements had little or no interferences from surfaces, where “room” burns are known to be compromised by the loss of materials, such as NH_3 , to the room walls at long sample times (Stockwell et al., 2014). Ash analyses were performed only on the residues from the room burns and those values will be used for the N and C budget calculations, with the assumption that stack and room burns left similar ash considering the combustion conditions were the same for each type of fire. Table 1 lists the compounds and associated techniques used to measure them during the FireLab 2016 study, and describes the grouping of NVOCs measured by PTR-ToF into common categories, e.g. amines, nitriles, etc.

2.1 N_r and NO measurements by Chemiluminescence

Total reactive N (N_r) was measured by catalytic conversion to NO, followed by O_3 -chemiluminescence using an instrument described previously (Williams et al., 1998). N_r and NO were sampled from inlets inserted adjacent to the inlet-less open-path Fourier transform infrared spectrometer (OP-FTIR) instrument path during the stack burns (Selimovic et al., 2018), and from a platform approximately 4 m off the floor in the middle of the room during the room burns. The catalyst used for the N_r channel, described in detail by Stockwell et al. (2018), consisted of a 11mm I.D. quartz tube, packed with 36 platinum screens, heated to 750°C. This tube was wrapped with high temperature heating tape and insulated inside a 7cm OD stainless steel tube that was fitted to a bulkhead placed through the wall



of the stack. The N_r channel was diluted by a factor of 5:1 ($\pm 3\%$) using a flow of zero air added immediately downstream of the Pt catalyst assembly. NO was sampled through a 6.3mm O.D. stainless steel inlet tube which was placed through the bulkhead directly into the free air stream of the stack and connected to a 50mm Teflon filter holder immediately outside the stack. The transfer lines for the N_r and NO measurements consisted of 6.35mm O.D, 1mm wall thickness PFA tubing of approximately 20 m in length. N_r and NO data were acquired at 1 s frequency, but the flow rate through each inlet was 1 SL min^{-1} , resulting in residence time in each inlet of 14 s. This time delay was corrected in the data analysis. Any chemical effects of the inlet on the sampled air stream were negligible since the analytes consisted of only NO and NO_2 and those are known to be transmitted by PFA Teflon tubing with essentially no surface effects. However, there were possible effects of the inlets on the temporal features of the measurement through diffusion or turbulent mixing. Those effects were examined through comparison of the temporal variations in the NO signal with the NO measured by the OP-FTIR, and comparison of the N_r signal under smoldering conditions with the NH_3 measured by the OP-FTIR. Both of these comparisons showed that the NO and N_r inlets had effective time constants of 4 seconds, somewhat slower than the diffusive relaxation time assuming solely laminar flow.

The inlet streams were sampled into the NO instrument either directly (NO channel) or after passing through a second catalyst of molybdenum oxide (MoOx) to convert remaining NO_2 to NO. The MoOx catalyst consisted of a molybdenum tube at 350°C to which a small flow of H_2 (0.8%v/v) was added to control the re-dox state of the surface. Both channels of the instrument were “de-tuned” to keep raw photon count rates below 4 MHz, by turning down the O_3 flows and PMT voltages. Calibrations were performed with both a NO standard in N_2 (Scott-Marrin) and 10.1 ppmv standard of HCN in nitrogen (Gasco). The Pt catalyst was dismounted from the stack (or room) every few days and checked for conversion efficiency by the addition of the HCN standard to the inlet. Conversion efficiencies were found to be consistently high ($>98\%$) throughout the entire sampling period (October 5 – November 12, 2016). There were slight background signals (a few tens of ppbv) for both NO and N_r in both the stack and room air prior to and after the burns, and those were subtracted from the fires signals prior to reporting the data. The overall uncertainties in the NO and N_r data were $\pm 10\%$ for each measurement.

2.2 Other measurements

Measurements of individual species during the 2016 FireLab study have been presented in several previous publications. The OP-FTIR measurements were discussed by Selimovic et al., 2018, and the PTR-ToF measurements were discussed by Koss et al., (2018). In addition, some of the calibration methods and GC separation and identifications rely on additional analytical work presented by Sekimoto et al., (2017) and Gilman et al., (2015). We measured the mass and elemental content of the initial fuel and the mass of unburned fuel for all the fires, and we measured the mass and the elemental content of the ash during 21 room burns, which covered all the fuel types discussed.

2.3 PMF Analysis

Trace gas measurements from multiple instruments involved in the FireLab study were combined and analyzed using positive matrix factorization (PMF). PMF is a numerical method that was used in this case to partition



the compounds involved in a time varying mixture of chemicals into a few groups, or “factors”, where a compound can appear in more than one factor. A factor represents a consistent profile of compounds that is representative of one of the sources contributing to the total signal. The sum of all the “factors” then ideally describes the total composition of the measurements, which in this case is the emissions of N_r compounds. By its nature, PMF assumes that the total signal is a linear combination of individual sources that have a consistent composition, the relative contribution of which is represented by the amount of each compound or category found in each factor (Paatero and Tapper, 1994; Ulbrich et al., 2009). We hypothesize that species with dominant fractions in the same factor are related to each other via the same formation processes. With knowledge of factor composition and the amount of each factor at any given time the original emissions measurements can be reconstructed and this approach provides an alternate source of profiles for fire emissions. PMF has also been used by a number of groups to explore how much various source profiles contribute to complex ambient measurements (see for example Ulbrich et al., 2009) and was recently used to analyze PTR-ToF-MS measurements from the FireLab (Sekimoto et al., 2018). Here, PMF was accomplished using the PMF Evaluation Tool v. 2.08A (Ulbrich et al., 2009).

The application of PMF to this data set is different than the instances where it is applied to data from a single instrument in which compound abundances are inherently scaled properly and error estimates are well defined and self-consistent. For example, when applied to mass spectral data from a single instrument, errors can be expected to scale as the square root of ion counts based on fundamental counting statistics (Sekimoto et al., 2018). In this work we are including nitrogen measurements from several instruments, thus we chose to use mixing ratios as the unit of comparison. The error estimates required by the PMF analysis were taken from the reported combined uncertainties: the sum of the detection limit plus the estimated random error of the measured value. The variables that were used in this PMF analysis and their units and corresponding errors are listed in Table 2. Where compound categories are specified (e.g. nitriles), the values were the sum of the measured compounds in that category as listed in the footnotes to Table 1. The data were further adjusted by subtracting the ambient air background before and after the fires, which was a relatively minor adjustment for most compounds and categories. Any negative numbers that resulted were very small compared to the fire emissions, and were set to zero.

Two approaches were taken when performing PMF analyses. The first approach included all individual N_r -containing compounds together with CO_2 , CO , and N_r in the analysis batch (Batch 1), while the second excluded the latter three species (Batch 2). CO_2 and CO were included because of their well-known roles as indicators of flaming and smoldering combustion, respectively, an effect traditionally captured through the use of Modified Combustion Efficiency (MCE) defined as

$$MCE = \Delta CO_2 / (\Delta CO_2 + \Delta CO) \quad (\text{Eq. 1})$$

where ΔCO_2 and ΔCO are the CO_2 and CO levels above the ambient. When CO_2 and CO were included, the carbon species were put into the PMF in units of ppmv, and all the nitrogen species in units of ppbv. This was done because the nitrogen levels were on the order of a percent or less compared to the carbon species. The second analysis batch (Batch 2) involved only the individually-measured nitrogen species and categories listed in Table 1 so that factor



loadings would be reflective of the nitrogen-only emissions. Batch 2 factors indicate how N_r species are related to each other via combustion chemistry.

We applied PMF to single fire data as well as extended time series that included all fires of a particular fuel type, in-line with the approach laid out by (Sekimoto et al., 2018). By consolidating fuels from a particular vegetation type, the fire to fire variability largely driven by differences in the fuel (e.g. moisture content, structure, quantity) is constrained and the most representative fire conditions are captured. Two fuel groups were analyzed in this way: the western U.S. coniferous ecosystem fuels which included ponderosa pine, lodgepole pine, Douglas fir, Engelmann spruce, and sub-alpine fir and the chaparral ecosystem which was represented by chamise and manzanita. The consolidated time series for the coniferous ecosystems included realistic mixtures, canopy only, and litter only, while duff and rotten logs were analyzed separately, and not included in the timeseries.

3 Results and Discussion

Example timeseries of NO , N_r , ΔCO , ΔCO_2 (CO and CO_2 corrected for their backgrounds) are shown in Figure 2, for a fire burning a sample of ponderosa pine realistic mix (Fire 004). MCE was also plotted in addition to the chemical species. The timeseries for Fire 004 shows a short initial smoldering/distillation phase (MCE 0.7 to 0.8) as heat pyrolyzes the fresh fuel and releases VOCs from exsiting pools in the fuel followed after ignition by a relatively efficient mix of flaming and smoldering combustion (MCE 0.95 to 0.98) and then finally a subsequent period of essentially pure smoldering (MCE ~ 0.80). The N_r and NO timelines had many features in common because NO is often the most abundant N_r compound (see below). As a result, it is useful to compare the quantities N_r - NO and $(N_r-NO)/N_r$ to the other measures of chemical species or combustion efficiency. As expected, $(N_r-NO)/N_r$ in Figure 2(c) is anti-correlated with MCE since N_r is primarily NO at high MCE. In addition to the anti-correlation, this non- NO fraction, like its approximate carbon analog CO/CO_2 , has a wider dynamic range than MCE and will often suffer less from background variability than carbon-based indices (Yokelson et al., 2013a).

The concentration profiles of the background-corrected measurements of N_r , CO_2 , CO , and all the carbon-containing species measured by the FTIR (Selimovic et al., 2018) during the stack burns were integrated over the entire time of the burn to obtain total carbon, termed TC here, and total N_r . The additional carbon species included methane and a number of other gas phase VOCs as well as organic- and black-carbon aerosol. Altogether these carbon species should account for $\geq 98\%$ of emitted carbon (McMeeking et al., 2009). Total N_r is plotted in Figure 3, versus TC (Figure 3a) and versus nitrogen burned, which is calculated from the %N in the fuel times the mass of fuel consumed (Figure 3b). The points in Figure 3 are colored by the fuel N/C mole % obtained from the elemental analysis of each fuel. The relationship between N_r and TC in panel 3a clusters around the 0.37% line and those points are from fuels most characteristic of the North American biomes impacted by wildfire. There are clear outliers in the correlation of N_r and TC; for example, yak dung and two samples of duff were high due either to the fact that they have high fuel N/C ratios, or they burned with minimal flaming (whole fire MCEs 0.86-0.89), hence experienced less de-nitrification. The fuels that were low in N_r /TC in panel 3a, ponderosa pine rotten log, subalpine fir and excelsior, had low fuel N/C, so when plotted versus nitrogen burned in panel 3b, they cluster with the main group of characteristic fuels, i.e. they are no longer 'outliers' in the distribution.



266 The points in Figure 3a are all lower than the corresponding fuel N/C mole ratio, due to the denitrification
 267 chemistry, shown in Figure 1, and verified in lab studies described by Kuhlbusch et al. (1991), and the production of
 268 N₂O which is also not measured by the N_r technique. The sum of N₂ and N₂O produced in the fires can be estimated
 269 from the difference between the fuel N/C and the N_r/Total C emitted and the data on C and N content remaining in
 270 the ash. The mass balance equations used for these calculations are detailed in the Supplemental Materials.

271 The distribution of the N lost to N₂ and N₂O is shown in Figure 4. Chemical analyses were not done for all
 272 fuels during the stack burns, and the analysis above assumes that the ash residues and ash/burned fuel ratios from the
 273 stack burns were well represented by those for the same fuels used in the room burns, for which mass yields and
 274 chemical analyses were done. Data are missing for fuels that did not have a corresponding ash analysis. The median
 275 fraction of N lost to N₂ and N₂O for ash-corrected fires was 0.70, and the mean (\pm standard deviation) was 0.68 (\pm 0.14).
 276 This fuel-based estimate is uncertain by approximately 25% because of the above assumptions concerning the
 277 applicability of the ash analyses from the room burns and because fuel moisture corrections were assumed to apply to
 278 all of the materials burned, foliage vs. woody biomass (see SI for details). The emission of N₂O relative to N₂ is
 279 approximately 10% or less for a wide range of fuels (Andreae, 2019). Assuming the N remainder in our work is at
 280 least 90% N₂ gives values that are somewhat higher than the N₂ values reported by Kuhlbusch et al., (1991) where N₂
 281 accounted for 36% of fuel N burned in flaming stage fires. A closer inspection of Kuhlbusch et al., (1991) showed a
 282 range of N₂ yields of 40-54% at highest MCEs of 0.94-0.97. Possible reasons for these differences are that the
 283 Kuhlbusch et al., (1991) fires were limited to grasses, hay, and pine needles, and the fires were confined to a closed
 284 container and so may not have experienced the convection and turbulence of typical biomass fires. In addition, the
 285 fires analyzed in our work were somewhat weighted towards the full canopy and higher temperature burning fuels,
 286 since ash analyses were not done for peat, dung and many of the “litter” samples, all of which tend to burn less
 287 efficiently. Goode et al., (1999) estimated an N₂ emission of 45 \pm 5% for MCE values of 0.95 in grass and surface fuels.
 288 The range of values determined in our work overlap with these literature values, but are on average higher. It should
 289 be noted that such loss of reactive nitrogen can have implications for ecosystem N budgets, as discussed by Kuhlbusch
 290 et al., (1991).

291 The composition of the N that does not get converted to N₂ or N₂O is of intense importance in determining
 292 atmospheric impacts of fires. Emission factors for all the individual N_r compounds identified in our work have been
 293 compiled and reported in previous publications (Koss et al., 2018; Selimovic et al., 2018), so this paper will focus on
 294 the N_r budget. The balance of N_r budget for Fire 047, sub-alpine fir realistic mix, is shown in Figure 5, in which the
 295 timelines of N_r, NO, N_r-NO, sumN, and NVOC are plotted along with MCE and (N_r-NO)/N_r. The quantity sumN is
 296 the sum of all other non-NO compounds, and NVOC is the subset of sumN that are organic nitrogen compounds
 297 measured by the PTR-ToF, as listed in Table 1. This fire had a mixture of flaming and smoldering combustion
 298 throughout the fire as indicated by MCE and nitrogen profiles (panel (d)). The comparison of N_r-NO with the sumN
 299 in panel (b) shows that much of the N is accounted for. The major contributors to sumN for this fire were HNCN,
 300 HCN, HONO, NO₂, and NH₃, while NVOC was a very small contributor to sumN (panel (b)). Note that while HNO₃
 301 is measurable by FTIR with good sensitivity, no HNO₃ signals were observed above detection limit, which was a few
 302 ppbv. Panel (c) shows the residual left after NO and sumN are subtracted from N_r, corresponding to an integrated



amount of $15.6 \pm 8\%$ of N_r . This residual is reasonable considering typical published particle N_r measurements (Akagi et al., 2012; Akagi et al., 2011; Liu et al., 2017; May et al., 2014), and consistent with there being some particle N_r from flaming, which are most likely organic nitrates or nitro-organics, and particle ammonium from smoldering with potassium or ammonium nitrate potentially accounting for substantial N_r .

In contrast to the above, the nitrogen emissions from Fire 050, yak dung, are shown in Figure 6. This fuel produced mostly smoldering emissions as exemplified by the low NO levels relative to N_r (panel a), and the low MCEs observed (panel d). The sum of N_r species was somewhat correlated with the quantity $N_r\text{-NO}$, but was substantially lower, and the residual N_r unaccounted for by the gas-phase measurements was $33.9 \pm 16\%$ of N_r (panel c). The majority of sumN was represented by HCN and NH_3 , with acetonitrile (CH_3CN) higher than any of the other inorganics, HNCN, NO_2 or HONO. The NVOCs were also a larger fraction of $N_r\text{-NO}$ than in the case of Fire 047 shown above, a feature that implies that more semi-volatile organic compounds, SVOC, survive these types of fires and could make a proportionally higher contribution to the N_r budget in this fire relative to Fire 047. FireLab results of particle organic carbon measurements (Jen et al., 2019) and field measurements in environments with a lot of dung burning (Jayarathne et al., 2018; Stockwell et al., 2016a) are consistent with a higher EF for particle organic carbon and by extension particle NVOC compounds. The quantity $(N_r\text{-NO})/N_r$ was relatively high and had less dynamic range than for fires with more flaming combustion like Fire 047.

The fire-integrated measurements of inorganic and NVOC species are listed in the Supplemental section as ratios to N_r for each stack fire (Table S1). The summary of all the fire integrated X_i/N_r fractions (where X_i is the N_r species or quantity) is given in Table 3 for all the fires for which we have a complete set of measurements (43 fires). In general, NO was the major species followed by NH_3 , and the other inorganic N_r species, NO_2 , HNCN, HONO, and HCN had individual contributions of 4.3 to 9.4 %. NVOC species were less than 5% of N_r on average. The unaccounted-for N_r , defined as $(N_r\text{-NO-sumN})/N_r$ had a median value of 14.3% and a mean (\pm std. dev.) of 15 (± 10)%. Overall, 85% of N_r was accounted for by the gas phase measurements. The distribution of whole fire N_r residuals is plotted as a histogram in Figure 7. We expect the residual N_r was composed of either semi- or low-volatility compounds, or particle-bound N_r compounds, which we know are converted efficiently by the N_r catalyst (Stockwell et al., 2018) but not detected by the instruments included in this analysis. Along these lines, there is some indication that the residual has a systematic variation with whole fire MCE, with higher residuals (up to 30%) observed at lower MCEs and higher $(N_r\text{-NO})/N_r$ (see Figure S1 a&b), which would be consistent with higher EF for SVOC at low MCE (Jen et al., 2019) and particle N_r having a higher contribution from NO_3^- (May et al., 2014), and perhaps particle ammonium or reduced- N_r compounds. In general, there is more particulate organic material emitted from fires at low MCE (Jen et al., 2019), so we would expect more particle N at low MCE to go along with that.

3.1 Systematic dependences of N_r composition on combustion processes.

The features noted in fires shown above, as well as the anti-correlation of MCE and $(N_r\text{-NO})/N_r$ lead to the question of whether there are systematic dependences in N_r -compound composition on fire stage that can be used to formally classify and/or potentially predict the relative emissions of N_r compounds. MCE has been used as a rough indicator of the relative amounts of flaming and smoldering combustion in a fire, with high MCE ($\sim 99\%$) being “pure”



flaming, low MCE (~80%) being “pure smoldering,” and an MCE of ~0.9 being roughly equal amounts of both (Sect. 2.1.1 in Akagi et al., 2011). It should be understood that “smoldering” in this framework is a lumped term that includes all non-flame processes such as pyrolysis, glowing, and distillation, while flames cannot exist without these processes producing gaseous fuel to support them (Yokelson et al., 1996). In addition, “pure flaming” is essentially the efficient oxidation of smoldering products before they enter the atmosphere. However, for MCE to predict flaming and smoldering N_r species well, the variable fuel N must be considered. For instance, NO_x is clearly produced by flaming based on its temporal profile, but fire-integrated EF_{NO_x} may not correlate with MCE due to variable fuel N. In these cases, $EF_{NO_x}/\text{fuel N}$ or $\Delta NH_3/\Delta NO_x$ may still correlate (or anti-correlate) well with MCE (e.g. Fig. 4 in Burling et al., 2010 or Yokelson et al., 1996). Finally, the flame chemistry involving NH_3 , $HNCO$, and HCN both produces and destroys NO in a fashion that does not conserve N_r . This chemistry is explored in Figure 8 in which NO_x , NH_3 , $HNCO$, HCN , $HONO$, and CH_3CN ratios to N_r are plotted vs real-time MCE for Fire 047 as a typical example for fires that have a substantial range of MCEs (e.g. from 0.8 to above 0.98). The relationship between NH_3/N_r and MCE confirms that NH_3 is primarily a smoldering emission and NO_x/N_r increases with increasing MCE in a non-linear fashion that confirms it is primarily a flaming compound. Such a non-linear dependence has also been seen for other flaming-related quantities such as Elemental Carbon/TC or EF_{HCl} (Christian et al 2003; Stockwell et al., 2014). Most importantly, the variations of $HNCO/N_r$, HCN/N_r , $HONO/N_r$, and CH_3CN/N_r versus MCE don’t arise dominantly from either regime as these are species that are likely produced by multiple pathways (e.g. “incomplete flaming”, pyrolysis, possibly glowing). By “incomplete” flame chemistry we mean the production of incompletely oxidized products in flames such as the complex system of reactions shown in Fig. 1. These reactions involving $HNCO$, HCN and NH_3 both produce and destroy NO , while $HONO$ is produced from reactions of NO and NO_2 that are faster at slightly lower temperatures, for example the three-body association reaction of NO with OH radical (Manion et al., 2015). Variable turbulence in the turbulent diffusion flames that are characteristic of open BB likely contributes to varying temperatures, and therefore, varying amounts of incomplete oxidation of the fuel N (Shaddix et al., 1994).

The complexity of the dependence of N_r speciation on combustion chemistry suggests that MCE is an insufficient model to use for applying lab results to real-world fire emissions (Stockwell et al., 2016a; Yokelson et al., 2013b). Accordingly, we employed the positive matrix factorization (PMF) method (see Methodology section) that has been used by a number of groups to probe the sources contributing to complex mixtures (see for example Ulbrich et al., 2009; Sekimoto et al., 2018). Our PMF results showed several general features, irrespective of the inclusion or exclusion of CO_2 , CO and N_r . The emissions were best fit by three factors (with approximate descriptive names justified below and prime species): (1) a combustion (flaming) factor (abbreviated Comb-N), (2) a high temperature pyrolysis factor (HT-N), and (3) a low temperature pyrolysis factor, (LT-N). We use these terms in part to harmonize our discussion with the VOC results discussed by Sekimoto 2018. An example timeseries for the PMF analysis of a coniferous fuel with just the N_r species included is shown in Figure 9 for a realistic mix of lodgepole pine (Fire 063), and Figure S2 shows the consolidated time series of all coniferous fuels fit using just the N_r species. The three factors successfully describe the majority of the N_r -emissions where the difference between the measured and calculated mass is on average 5.1% for coniferous fuels and 4.6% for chaparrals as indicated in Table 4.



The ‘loadings’ of the three different factors, i.e. the contribution of compounds to each factor, for coniferous fuels are shown in Figure 10(a), and the distribution of a given compound or compound class amongst the three factors is shown in Figure 10(b) as normalized fraction. Normalized fraction is equal to the PMF-determined contribution of a compound to a factor, divided by the sum of the contribution of the compound to all three factors. The Comb-N factor contained NO, NO₂, and HONO, the HT-N factor had mostly HCN, HNCO, nitriles, with contributions from NO₂ and nitro compounds, and the LT-N factor contained NH₃, amines, amides and heterocyclics. Within the Comb-N factor there is some evidence that the relative amounts of HONO and NO_x depend on fuel moisture. For example, the ratio HONO/NO_x for whole fires shows some correlation with needle moisture in coniferous fires that were canopy fuels (Foliage and small woody biomass), as shown in Figure S3. This may be due to flame process the interconvert NO_x and HONO in the presence of water vapor of OH (see Figure 1).

Literature values from studies where flame temperature was measured are typically in the range of 1100 – 1200 °C (Taylor et al., 2004; Wotton et al., 2012), so we would assume that would constitute the upper range of our Comb-N factor. The radical chemistry involving HCN, HNCO and NH₃ starts to shut down below about 800-900°, according to the modeling of Glarborg et al., (2018), so we set 800°C as a lower limit for the Comb-N factor. The HT-N factor species are known to be produced by the intense pyrolysis of fuel N_r compounds (Hansson et al., 2004; Liu et al., 2018; Ren et al., 2010), which for these compounds becomes important at temperatures around 500-600°C. Accordingly, we estimate the temperature range for the HT-N factor at 500 – 800°C. The remaining LT-N factor results from mild pyrolysis and pertains to fire conditions of roughly 500°C and below, and was dominated by NH₃, amines, amides and some of the more complex organics (Koss et al., 2018). The names and temperature ranges are approximate and likely include processes that occur inside flames as part of the flame proper, as turbulent diffusive flames are highly variable in space and time.

It is useful to explore the correlation of N-PMF factors with other fire indicators to determine relationships for parameterizing N_r emissions together with carbon and VOC emissions. The Comb-N factor for coniferous fuels, which consisted of NO_x and HONO, would be expected to correlate with CO₂ but not as well with MCE since the latter includes an indicator of incomplete combustion. The timeseries of Comb-N along with CO₂ and with MCE for Fire 037 (ponderosa pine), are plotted in Figure 11. As expected they show an excellent correlation of Comb-N with CO₂ ($R^2=0.942$) since all the species are flaming compounds, but non-linear correlation of Comb-N with MCE ($R^2=0.363$) since the latter factors in a smoldering compound (CO), similar to the NO_x/N_r vs. MCE plot for Fire 047 in Figure 8. The excellent correlation of Comb-N with CO₂ is a broadly applicable result, the R^2 parameters for all the fires shown in Figure S2 had an average of 0.898, and ranged from 0.806 to 0.966. As a consequence, we can conclude that CO₂ would be the best tracer for Comb-N in many western U.S. ecosystems where conifers predominate, provided ambient CO₂ backgrounds can be properly accounted for as described by Yokelson et al., (2013a).

Our Comb-N factor did not correspond to the high temperature VOC factor (HT-VOC) found by Sekimoto et al., (2018), because combustion produces NO_x, and HONO, but almost none of the compounds classified as VOCs survive these conditions. However, the HT-N and HT-VOC factors were well correlated for many fires. An example of this is shown in Figure 12 for Fire 037, a sample that was broadly representative of ponderosa pine (i.e. canopy and litter). This result can be rationalized by the fact that while HT-VOC factors have large contributions from many more



compounds that the N compounds measured here, they also have large contributions (>85%) from HCN, HNCO, and HONO, (in other words >85% of HCN, HNCO and HONO are found in the HT-VOC factor). Since the HT-N factors are also heavily weighted by HCN and HNCO, it is reassuring that both of these PMF analyses have independently identified these species as important contributors to the HT fire regime. The R^2 correlation coefficients of HT factors for the coniferous shown in Figure S2 averaged 0.866 and ranged from 0.419 to 0.959. As a consequence of this correlation, we can conclude that HCN is the best marker for the HT-N and HT-VOC factors in most western U.S. wildfires, since HCN is essentially inert on the timescales of fire plumes.

The correlations of LT-N and LT-VOC factors were not particularly high for most of the coniferous fires shown in Figure S2. The average R^2 was 0.427 with a range of between 0.072 and 0.827. The reasons for this lack of correlation are not clear, as NH_3 , amines and amides appear predominantly in both LT factors, and the absolute concentrations of NH_3 are usually quite high in these fires relative to VOCs (Sekimoto et al., 2018). However, the LT-VOC factor includes many more compounds with a variety of functional groups not found in the LT-N factor, so it appears that the VOC and N compounds have sufficiently different pyrolysis chemistry that the LT factors do not show much correlation. We conclude that NH_3 (and particle NH_4^+) will be the best marker for the LT-N factor in western U.S. coniferous wildfires, but the LT-VOC chemistry might not be captured reliably by this marker.

The emissions from burning chaparral fuels (manzanita and chamise) collected at two sites in California were also analyzed as a group and yielded three separate factors in a fashion similar to the coniferous fuels (see Figure S4 for the PMF timeline). The chaparral factors had slightly different composition (Figure S5), the combustion factor was mostly NO, with small amounts of HNCO, HONO and NH_3 , the high temperature factor was dominated by NO_2 and included HONO, HCN, and HNCO, and the low temperature factor was mostly NH_3 with a slight amount of NO contributing. The NVOC species were found in both the medium and low temperature factors.

There was less similarity between the Comb-N factor and CO_2 emissions for chaparral fuels compared to those found for coniferous fuels, with an average correlation coefficient (R^2) of 0.689, with a range from 0.244 and 0.950. As a result, there may not be a simple conserved tracer for the combustion factor of these fuel types, however total odd nitrogen (NO_y) which is NO_x and all the compounds that are produced from NO_x in the troposphere, may be useful as it is a reasonably conserved tracer in the absence of wet or dry deposition of particles. Correlation coefficients between the HT-N and HT-VOC factors were on average $R^2 = 0.551$, with a range 0.047-0.911. The correlations between LT-N and LT-VOC factors were in the same range for chaparral fuels as for coniferous, average $R^2 = 0.447$, range 0.028-0.827.

There were some fuels that do not sustain flaming combustion well, specifically duff, Yak dung and Indonesian peat. These fires exhibited little or no NO emission commensurate with minimal flaming combustion. Instead the emissions were mostly the pyrolysis products NH_3 , (0.22 – 0.53 N_r fraction), and HCN (up to 0.32 N_r fraction for peat). It was also apparent that these fires also had unaccounted for N_r , close to, or just over 0.30 (Table S1). The distribution of N_r compounds in the one peat fire that we measured (Fire 055) is in line with those reported for fires measured in situ which showed relatively high EFs for HCN and NH_3 (Stockwell et al., 2016b; Stockwell et al., 2015).



The application of our N_r emissions results to real-world fires will depend somewhat on the nature of the information available on a particular fire, or fire complex. As a good starting point, or in the absence of detailed N and C analyses of fuels, a N_r/C ratio of 0.37% appears to capture most of the fires studied in this work. The N_r can be apportioned according to the results summarized in Table 3. Adjustments to those fractions can be made either by scaling slightly by average MCE, with the knowledge that intermediate species (HT-N pyrolysis species) such as HCN and HNCO do not scale in the simple manner that NH_3 and NO_x do. If measurements of marker compounds are available then CO_2 , HCN, and the sum $NH_3 + NH_4^+$ can be used for the combustion, high-temperature pyrolysis, and low-temperature pyrolysis factors respectively.

4 Conclusions

Seventy-five stack fire experiments were conducted during the FIREX FireLab experiments in Fall, 2016. A range of fuels characteristic of the western U.S. was burned under conditions and in mixtures meant to represent authentic wildfire conditions, as closely as is possible in the laboratory. Total reactive nitrogen (N_r = all N-containing compounds except N_2 and N_2O) was measured along with a suite of N-containing compounds in order to obtain a budget for N_r -emissions and to examine relationships between fuels, combustion conditions, and emissions chemistry.

Natural convection wildfires do not burn hot enough to produce NO_x from N_2 and O_2 , so all N_r emissions come from the fuel N. Almost all of the fires representative of North American ecosystems had emissions that clustered around a N_r/C ratio of 0.37%, which can serve as a starting point for scaling emissions from these ecosystems. Comparison total N_r and total carbon emissions with the N/C ratios of both the original fuel and remaining ash allowed us to estimate that an average of 68% ($\pm 14\%$) of the fuel nitrogen ends up as N_2 and N_2O . This loss of nitrogen can be used to estimate how much fuel nitrogen ends up as N_r , which is a crucial aspect of fire plume chemistry since the photo chemistry many fire plumes is NO_x -limited, and NH_3 is an important contributor to particle chemistry. Of the remaining N emitted as N_r , approximately 85% ($\pm 10\%$) was accounted for by individually measured gas-phase species, while the rest was most likely particle-bound NH_4^+ and NO_3^- , with a smaller contribution from low-volatility species or other species such as cyanogen (Lobert and Warnatz, 1993), that were not quantified by the instruments for individual measurements we used in this study.

The individual N_r species composition normalized to Total N_r , to account for fuel N variability, correlated with flaming versus vs. smoldering combustion as indicated by modified combustion efficiency (MCE) for some species (e.g. NH_3 , NO_x). Other species, such as HCN and HNCO, peaked at intermediate MCE values. However, positive matrix factorization (PMF) showed that all the measured N_r emissions from the main two categories of fuels, conifers and chaparral, grouped into three mixtures (factors), roughly attributed to temperature: combustion (NO_x , HONO), high temperature (HNCO, HCN, nitriles), and low temperature (NH_3 , amines, amides). Chemical kinetic and pyrolysis considerations set the temperature ranges for these regimes at approximately 800-1200°C, 500-800°C and <500°C respectively.

This paper connects mechanistic aspects of N combustion chemistry to the budget of N_r emissions from biomass burning. The emission composition measurements detailed here give useful information concerning what the initial conditions will be in actual fire plumes. These results suggest that for coniferous fuels characteristic of the



western U.S. CO₂ is the best marker for flaming combustion, HCN is the best marker for high temperature pyrolysis processes, and NH₃/NH₄⁺ is the best marker for low temperature pyrolysis processes. The HT-N and HT-VOC pyrolysis factors showed high degree of correlation especially for coniferous fuels, which can simplify how these different classes of emissions can be estimated. Results of future field intensives can be combined with this emissions information to refine these recommendations on how to put N₂-chemistry into the modeling frameworks needed to predict fire plume chemistry and impacts.

492

493 Data availability

494 The FIREX Firelab 2016 data are available at:
 495 <https://esrl.noaa.gov/csd/groups/csd7/measurements/2016firex/FireLab/DataDownload/>. The descriptions of the
 496 measurements can be found here:
 497 <https://esrl.noaa.gov/csd/groups/csd7/measurements/2016firex/FireLab/dataidtable.html>. The complete ash analyses
 498 are available on request.
 499

500 Author Contributions

501 JMR, RY, CW and JdG designed the research. The measurements were conducted by JMR, CS, CW, RJY,
 502 JdG, YL, VS, ARK, KS, MMC, BY, KJZ, SSB, CS, and SHD. All authors contributed to the discussion and
 503 interpretation of the results and writing the paper.
 504

505 Competing interests

506 Joost de Gouw worked as a consultant for Aerodyne Research during part of the preparation phase of this
 507 paper.
 508

509 Disclaimer

510 Any mention of brand names or manufacturers is for information purposes only and does not constitute an
 511 endorsement.
 512

513 Acknowledgements

514 A. Koss acknowledges funding from the NSF Graduate Fellowship Program. K. Sekimoto acknowledges
 515 funding from the Postdoctoral Fellowships for Research Abroad from Japan Society for the Promotion of Science
 516 (JSPS) and a Grant-in-Aid for Young Scientists (B) (15K16117) from the Ministry of Education, Culture, Sports,
 517 Science and Technology of Japan. R. Yokelson and V. Selimovic were supported by NOAA-CPO grant
 518 NA16OAR4310100. J. de Gouw was supported by the NSF AGS grant 1748266 under a subcontract to the University
 519 of Montana during the analysis phase of this work. We thank the USFS Missoula Fire Sciences Laboratory for their
 520 help in conducting these experiments, especially Shawn Urbanski and Thomas Dzomba. This work was also supported
 521 by NOAA's Climate Research and Health of the Atmosphere Initiative.
 522

523 References

524
 525 Abatzoglou, J. T. and Williams, A. P.: Impact of anthropogenic climate change on wildfire across western US
 526 forests, *Proc. Natl. Acad. Sci.*, 113, 11770-11775, 2016.
 527
 528 Akagi, S. K., Craven, J. S., Taylor, J. W., McMeeking, G. R., Yokelson, R. J., Burling, I. R., Urbanski, S. P., Wold,
 529 C. E., Seinfeld, J. H., Coe, H., Alvarado, M. J., and Weise, D. R.: Evolution of trace gases and particles emitted by a
 530 chaparral fire in California, *Atmos. Chem. Phys.*, 12, 1397-1421, 2012.
 531



- 532 Akagi, S. K., Yokelson, R. J., Wiedinmyer, C., Alvarado, M. J., Reid, J. S., Karl, T., Crounse, J. D., and Wennberg,
 533 P. O.: Emission factors for open and domestic biomass burning for use in atmospheric models, *Atmos. Chem. Phys.*
 534 , 11, 4039-4072, 2011.
- 535
- 536 Alvarado, M. J., Logan, J. A., Mao, J., Apel, E., Riemer, D., Blake, D., Cohen, R. C., K.-E., M., Perring, A. E.,
 537 Browne, E. C., Wooldridge, P. J., Diskin, G. S., Sachse, G. W., Fuelberg, H., Sessions, W. R., Harrington, D. L.,
 538 Huey, L. G., Liao, J., Case-Hanks, A., Jimenez, J. L., Cubison, M. J., Vay, S. A., Weinheimer, A. J., Knapp, D. J.,
 539 Montzka, D. D., Flocke, F. M., Pollack, I. B., Wennberg, P. O., Kurten, A., Crounse, J. D., St. Clair, J. M.,
 540 Wisthaler, A., Mikoviny, T., Yantosca, R. M., Carouge, C. C., and Le Sager, P.: Nitrogen oxides and PAN in plumes
 541 from boreal fires during ARCTAS-B and their impact on ozone: an integrated analysis of aircraft and satellite
 542 observations, *Atmos. Chem. Phys.*, 10, 9739-9760., 2010.
- 543
- 544 Andreae, M. O.: Emission of trace gases and aerosols from biomass burning – an updated assessment, *Atmos.*
 545 *Chem. Phys.*, 19, 8523-8546, 2019.
- 546
- 547 Andreae, M. O. and Merlet, P.: Emission of trace gases and aerosols from biomass burning, *Global Biogeochem.*
 548 *Cycles*, 15, 955-966, 2001.
- 549
- 550 Benedict, K. B., Prenni, A. J., Carrico, C. M., Sullivan, A. P., Schichtel, B. A., and Collett Jr., J. L.: Enhanced
 551 concentrations of reactive nitrogen species in wildfire smoke, *Atmos Environ.*, 148, 8-15, 2017.
- 552
- 553 Burling, I. R., Yokelson, R. J., Griffith, D. W. T., Johnson, T. J., Veres, P., Roberts, J. M., Warneke, C., Urbanski,
 554 S. P., Reardon, J., Weise, D. R., Hao, W. M., and de Gouw, J.: Laboratory measurements of trace gas emissions
 555 from biomass burning of fuel types from the southeastern and southwestern United States, *Atmos. Chem. Phys.*, 10,
 556 11115-11130, 2010.
- 557
- 558 Christian, T. J., Kleiss, B., Yokelson, R. J., Holzinger, R., Crutzen, P. J., Hao, W. M., Shirai, T., and Blake, D. R.:
 559 Comprehensive laboratory measurements of biomass-burning emissions: 2, First intercomparison of open path
 560 FTIR, PTR-MS, GC-MS/FID/ECD, *J. Geophys. Res.*, 109, D02311, 2004.
- 561
- 562 Coggon, M., Veres, P. R., Yuan, B., Koss, A. R., Warneke, C., Gilman, J. B., Lerner, B., Peischl, J., Aikin, K.,
 563 Stockwell, C. E., Hatch, L. E., Ryerson, T. B., Roberts, J. M., Yokelson, R. J., and de Gouw, J.: Emissions of
 564 nitrogen-containing organic compounds from the burning of herbaceous and arboraceous biomass: fuel composition
 565 dependence and the variability of commonly used nitrile tracers, *Geophys. Res. Lett.*, 43, 9903-9912, 2016.
- 566
- 567 Crutzen, P. J. and Andreae, M. O.: Biomass burning in the tropics: Impact on atmospheric chemistry and
 568 biogeochemical cycles, *Science*, 250, 1669-1678, 1990.
- 569
- 570 Gilman, J. B., Lerner, B. M., Kuster, W. C., Goldan, P. D., Warneke, C., Veres, P. R., Roberts, J. M., deGouw, J. A.,
 571 Burling, I. R., and Yokelson, R. J.: Biomass burning emissions and potential air quality impacts of volatile organic
 572 compounds and other trace gases from temperate fuels common to the United States, *Atmos. Chem. Phys.*, 15,
 573 13915-13938, 2015.
- 574
- 575 Glarborg, P., Miller, J. A., Ruscic, B., and Klippenstein, S. J.: Modeling nitrogen chemistry in combustion, *Prog.*
 576 *Energy Comb. Sci.*, 67, 31-68, 2018.
- 577
- 578 Goode, J. G., Yokelson, R. J., Susott, R. A., and Ward, D. E.: Trace gas emissions from laboratory biomass fires
 579 measured by open-path Fourier transform infrared spectroscopy: Fires in grass and surface fuels *J. Geophys. Res.*,
 580 104, 21237-21245, 1999.
- 581
- 582 Griffith, D. W. T., Mankin, W. G., Coffey, M. T., Ward, R. E., and Riebau, A.: FTIR remote sensing of biomass
 583 burning emissions of CO₂, CO, CH₄, CH₂O, NO, NO₂, NH₃, and N₂O. In: *Global Biomass Burning: Atmospheric,*
 584 *Climatic, and Biospheric Implications*, Levine, J. S. (Ed.), The MIT Press, Cambridge, MA, 1991.
- 585
- 586 Hansson, K.-M., Samuelsson, J., Tullin, C., and Amand, L.-E.: Formation of HNCO, HCN, and NH₃ from the
 587 pyrolysis of bark and nitrogen-containing model compounds, *Combust. Flame*, 137, 265-277, 2004.



- 588
 589 Hao, W. M., Scharffe, D. H., Lobert, J. M., and Crutzen, P. J.: Emissions of N₂O from the burning of biomass in an
 590 experimental system, *Geophys. Res. Lett.*, 18, 999-1002, 1991.
 591
 592 Hardy, J. E. and Knarr, J. J.: Technique for measuring the total concentration of gaseous fixed nitrogen species, *J. Air*
 593 *Pollut. Contr. Assoc.*, 32, 376-379, 1982.
 594
 595 Jayarathne, T., Stockwell, C. E., Bhawe, P. V., Praveen, P. S., Rathnayake, C. M., Islam, M. R., Panday, A. K.,
 596 Adhikari, S., Maharjan, R., Goetz, J. D., DeCarlo, P. F., Saikawa, E., Yokelson, R. J., and Stone, E. A.: Nepal
 597 Ambient Monitoring and Source Testing Experiment (NAMaSTE): emissions of particulate matter from wood-
 598 dung-fueled cooking fires, garbage and crop residue burning, brick kilns, and other sources, *Atmos. Chem. Phys.*,
 599 doi: 10.5194/acp-18-2259-2018, 2018. 2259-2286, 2018.
 600 J
 601 en, C. N., Hatch, L. E., Selimovic, V., Yokelson, R. J., Weber, R., Fernandez, A. E., Kreisberg, N. M., Barsanti, K.
 602 C., and Goldstein, A. H.: Speciated and total emission factors of particulate organics from burning western US
 603 wildland fuels and their dependence on combustion efficiency, *Atmos. Chem. Phys.*, 19, 1013-1026, 2019.
 604
 605 Kashihiro, N., Makino, K., Kirita, K., and Watanabe, Y.: Chemiluminescent nitrogen detector-gas chromatography
 606 and its application to measurement of atmospheric ammonia and amines, *J. Chromatogr.*, 239, 617-624, 1982.
 607
 608 Koss, A. R., K., S., Gilman, J. B., Selimovic, V., Coggon, M. M., Zarzana, K. J., Yuan, B., Lerner, B. M., Brown, S.
 609 S., Jimenez, J. L., J., K., Roberts, J. M., Warneke, C., Yokelson, R. J., and de Gouw, J.: Non-methane organic gas
 610 emissions from biomass burning: identification, quantification, and emission factors from PTR-ToF during the
 611 FIREX 2016 laboratory experiment, *Atmos. Chem. Phys.*, 18, 3299-3319, 2018.
 612
 613 Kuhlbusch, T. A., Lobert, J. M., Crutzen, P. J., and Warneck, P.: Molecular nitrogen emissions from denitrification
 614 during biomass burning, *Nature*, 351, 135-137, 1991.
 615
 616 Lee, D. C., Quigley, T. M., Norman, S., Christie, W., Fox, J., Rogers, K., and Hutchins, M.: National Cohesive
 617 Wildland Fire Management Strategy, U.S. Department of the Interior, Washington, D.C., 2014.
 618
 619 Liu, X., Huey, L. G., Yokelson, R. J., Selimovic, V., I.J., S., Muller, M., Jimenez, J. L., Campuzano-Jost, P.,
 620 Beyersdorf, A. J., Blake, D. R., Butterfield, Z., Choi, Y., Crounse, J. D., Day, D. A., Diskin, G. S., Dubey, M. K.,
 621 Fortner, E., Hanisco, T. F., Hu, W., King, L. E., L., K., Meinardi, S., Mikoviny, T., Onasch, T. B., Palm, B. B.,
 622 Peischl, J., Pollack, I. B., Ryerson, T. B., Sachse, G. W., Sedlacek, A. J., Shilling, J. E., Springston, S. R., St. Clair,
 623 J. M., Tanner, D. J., Teng, A. P., Wennberg, P. O., Wisthaler, A., and Wolfe, G. M.: Airborne measurements of
 624 western U.S. wildfire emissions: Comparison with prescribed burning and air quality implications, *J. Geophys.*
 625 *Res.*, 122, 6108-6129, 2017.
 626
 627 Liu, X., Luo, Z., Yu, C., Jin, B., and Tu, H.: Release mechanism of fuel-N into NO_x and N₂O precursors during
 628 pyrolysis of rice straw, *Energies*, 11, 520, 2018.
 629
 630 Liu, X., Zhang, Y., Huey, L. G., Yokelson, R. J., Wang, Y., Jimenez, J. L., Campuzano-Jost, P., Beyersdorf, A. J.,
 631 Blake, D. R., Choi, Y., St. Clair, J. M., Crounse, J. D., Day, D. A., Diskin, G. S., Fried, A., Hall, S. R., Hanisco, T.
 632 F., King, L. E., Meinardi, S., Mikoviny, T., Palm, B. B., J., P., A.E., P., Pollack, I. B., Ryerson, T. B., Sachse, G.
 633 W., Schwarz, J. P., Simpson, I. J., Tanner, D. J., Thornhill, K. L., Ullman, K., Weber, R. J., Wennberg, P. O.,
 634 Wisthaler, A., Wolfe, G. M., and Ziemba, L. D.: Agricultural fires in the southeastern U.S. during SEAC⁴RS:
 635 Emissions of trace gases and particles and evolution of ozone, reactive nitrogen, and organic aerosol, *J. Geophys.*
 636 *Res.*, 121, 7383-7414, 2016.
 637
 638 Lobert, J. M., Scharffe, D. H., Hao, W.-M., Kuhlbusch, T. A., Seuwen, R., Warneck, P., and Crutzen, P. J.:
 639 Experimental evaluation of biomass burning emissions: Nitrogen and carbon containing compounds. In: *Global*
 640 *Biomass Burning: Atmospheric, Climatic, and Biospheric Implications*, Levine, J. S. (Ed.), The MIT Press,
 641 Cambridge, MA, 1991.
 642



- 643 Lobert, J. M., Scharffe, D. H., Hao, W. M., and Crutzen, P. J.: Importance of biomass burning in the atmospheric
 644 budgets of nitrogen-containing gases, *Nature*, 346, 552-554, 1990.
- 645
 646 Lobert, J. M. and Warnatz, J.: Emissions from the combustion process in vegetation. In: *Fire in the Environment:*
 647 *The Ecological, Atmospheric and Climatic Importance of Vegetation Fires*, Crutzen, P. J. and Goldammer, J. G.
 648 (Eds.), John Wiley and Sons, New York, N.Y., 1993.
- 649
 650 Lucassen, A., Zhang, K., Warkentin, J., Mashhammer, K., Glarborg, P., Marshall, P., and Kohse-Hoinghaus, K.:
 651 Fuel-nitrogen conversion in the combustion of small amines using dimethylamine and ethylamine as biomass-related
 652 model fuels, *Combust. Flame*, 159, 2254-2279, 2012.
- 653
 654 Manfred, K. M., Washenfelder, R. A., Wagner, N. L., Adler, G., Erdesz, F., Womack, C. C., Lamb, K. D., Schwarz,
 655 J. P., Franchin, A., Selimovic, V., Yokelson, R. J., and Murphy, D. M.: Investigating biomass burning aerosol
 656 morphology using a laser imaging nephelometer, *Atmos. Chem. Phys.*, 18, 1879-1894, 2018.
- 657
 658 Manion, J. A., Huie, R. E., Levin, R. D., Burgess Jr., D. R., Orkin, V. L., Tsang, W., McGivern, W. S., Hudgens, J.
 659 W., Knyazev, V. D., Atkinson, D. B., Cahill, E., Tereza, A. M., Lin, C.-Y., Allison, T. C., Mallard, W. G., Westley,
 660 F., Herron, J. T., Hampson, R. F., and Frizzell, D. H.: <http://kinetics.nist.gov/>, 2015.
- 661
 662 Marx, O., Brummer, C., Ammann, C., Wolff, V., and Freibauer, A.: TRANC – a novel fast-response converter to
 663 measure total reactive atmospheric nitrogen, *Atmos. Meas. Tech.*, 5, 1045-1057, 2012.
- 664
 665 May, A. A., McMeeking, G. R., Lee, T., Taylor, J. W., Craven, J. S., Burling, I. R., Sullivan, A. P., Akagi, S. K.,
 666 Collett, J. L. J., Flynn, M., Coe, H., Urbanski, S. P., Seinfeld, J. H., Yokelson, R. J., and Kreidenweis, S. M.:
 667 Aerosol emissions from prescribed fires in the United States: A synthesis of laboratory and aircraft measurements, *J.*
 668 *Geophys. Res.*, 119, 2014.
- 669
 670 McMeeking, G. R., Kreidenweis, S. M., Baker, S., Carrico, C. M., Chow, J. C., Collett Jr., J. L., Hao, W. M.,
 671 Holden, A. S., Kirchstetter, T. W., Malm, W. C., Moosmuller, H., Sullivan, A. P., and Wold, C. E.: Emissions of
 672 trace gases and aerosols during the open combustion of biomass in the laboratory, *J. Geophys. Res.*, 114,
 673 doi:10.1029/2009JD011836, 2009.
- 674
 675 NOAA: <https://www.esrl.noaa.gov/csd/projects/firex/2018>.
- 676
 677 Paatero, P. and Tapper, U.: Positive matrix factorization: A non-negative factor model with optimal utilization of
 678 error estimates of data values. , *Environmetrics*, 5, 111-126, 1994.
- 679
 680 Prenni, A. J., Levin, E. J. T., Benedict, K. B., Sullivan, A. P., Schurman, M. I., Gebhart, K. A., Day, D. E., Carrico,
 681 C. M., Malm, W. C., Schichtel, B. A., Collett Jr., J. L., and Kreidenweis, S. M.: Gas-phase reactive nitrogen near
 682 Grand Teton National Park: Impacts of transport, anthropogenic emissions, and biomass burning, *Atmos Environ.*,
 683 89, 749-756, 2014.
- 684
 685 Ren, Q. Q., Zhao, C. S., Wu, X. X., Liang, C., Chen, X. P., Shen, J. Z., and Wang, Z.: Formation of NO_x precursors
 686 during wheat straw pyrolysis and gasification with O₂ and CO₂, *Fuel*, 89, 1064-1069, 2010.
- 687
 688 Roberts, J. M., Langford, A. O., Goldan, P. D., and Fehsenfeld, F. C.: Ammonia measurements at Niwot Ridge,
 689 Colorado, and Point Arena, California, using the tungsten oxide denuder tube technique, *J. Atmos. Chem.*, 7, 137-
 690 152, 1988.
- 691
 692 Roberts, J. M., Veres, P. R., Cochran, A. K., Warneke, C., Burling, I. R., Yokelson, R. J., Lerner, B. M., Gilman, J.
 693 B., Kuster, W. C., Fall, R., and de Gouw, J.: Isocyanic acid in the atmosphere and its possible link to smoke-related
 694 health effects, *PNAS*, 108, 8966-8971, 2011.
- 695
 696 Saylor, R. D., Edgerton, E. S., Hartsell, B. E., Baumann, K., and Hansen, D. A.: Continuous gaseous and total
 697 ammonia measurements from the southeastern aerosol research and characterization (SEARCH) study, *Atmos.*
 698 *Environ.*, 44, 4994-5004, 2010.



- 699
 700 Schwab, J. J., Li, Y., Bae, M.-S., Demerjian, K. L., Hou, J., Zhou, X., Jensen, B., and Pryor, S.: A laboratory
 701 intercomparison of real-time gaseous ammonia measurement methods, *Environ. Sci. Technol.*, 41, 8412-8419,
 702 2007.
 703
 704 Sekimoto, K., Koss, A. R., Gilman, J. B., Selimovic, V., Coggon, M. M., Zarzana, K. J., Yuan, B., Lerner, B. M.,
 705 Brown, S. S., Warneke, C., Yokelson, R. J., Roberts, J. M., and de Gouw, J.: High- and low-temperature pyrolysis
 706 profiles describe primary emissions of volatile organic compounds from western US wildfire fuels, *Atmos. Chem.*
 707 *Phys.*, 18, 9263-9281, 2018.
 708
 709 Selimovic, V., Yokelson, R. J., Warneke, C., Roberts, J. M., deGouw, J. A., Reardon, J., and Griffith, D. W. T.:
 710 Aerosol optical properties and trace gas emissions by PAX and OP-FTIR for laboratory-simulated western US
 711 wildfires during FIREX, *Atmos. Chem. Phys.*, 18, 2929-2948, 2018.
 712
 713 Shaddix, C. R., Harrington, J. E., and Smyth, K. C.: Quantitative measurements of enhanced soot production in a
 714 flickering methane/air diffusion flame, *Combust. Flame*, 99, 723-732, 1994.
 715
 716 Stockwell, C. E., Christian, T. J., Goetz, J. D., Jayarathne, T., Bhawe, P. V., Praveen, P. S., Adhikari, S., Maharjan,
 717 R., DeCarlo, P. F., Stone, E. A., Saikawa, E., Blake, D. R., Simpson, I. J., Yokelson, R. J., and Panday, A. K.: Nepal
 718 Ambient Monitoring and Source Testing Experiment (NAMaSTE): emissions of trace gases and light-absorbing
 719 carbon from wood and dung cooking fires, garbage and crop residue burning, brick kilns, and other sources, *Atmos.*
 720 *Chem. Phys.*, 16, 11043-11081, 2016a.
 721
 722 Stockwell, C. E., Jayarathne, T., Cochrane, M. A., Ryan, K. C., Putra, E. I., Saharjo, B. H., Nurhayati, A. D., Albar,
 723 I., Blake, D. R., Simpson, I. J., Stone, E. A., and Yokelson, R. J.: Field measurements of trace gases and aerosols
 724 emitted by peat fires in Central Kalimantan, Indonesia, during the 2015 El Niño, *Atmos. Chem. Phys.*, 16, 11711 -
 725 11732, 2016b.
 726
 727 Stockwell, C. E., Kupc, A., Witkowski, B., Talukdar, R. K., Liu, Y., Selimovic, V., Zarzana, K. J., Sekimoto, K.,
 728 Warneke, C., Washenfelder, R. A., Yokelson, R. J., Middlebrook, A. M., and Roberts, J. M.: Characterization of a
 729 catalyst-based conversion technique to measure total particle nitrogen and organic carbon and comparison to a
 730 particle mass measurement instrument, *Atmos. Meas. Tech.*, 11, 2749-2768, 2018.
 731
 732 Stockwell, C. E., Veres, P. R., Williams, J., and Yokelson, R. J.: Characterization of biomass burning smoke from
 733 cooking fires, peat, crop residue and other fuels with high resolution proton-transfer-reaction time-of-flight mass
 734 spectrometry, *Atmos. Chem. Phys.*, 15, 845-865, 2015.
 735
 736 Stockwell, C. E., Yokelson, R. J., Kreidenweis, S. M., Robinson, A. L., DeMott, P. J., Sullivan, R. C., Reardon, J.,
 737 Ryan, K. C., Griffith, D. W. T., and Stevens, L.: Trace gas emissions from combustion of peat, crop residue,
 738 domestic biofuels, grasses, and other fuels: configuration and Fourier transform infrared (FTIR) component of the
 739 fourth Fire Lab at Missoula Experiment (FLAME-4), *Atmos. Chem. Phys.*, 14, 9727-9754, 2014.
 740
 741 Taylor, S. W., Wotton, B. M., Alexander, M. E., and Dalrymple, G. N.: Variation in wind and crown fire behaviour
 742 in a northern jack pine-black spruce forest, *Canadian J. Forest Res.*, 34, 1561-1576, 2004.
 743
 744 Ulbrich, I. M., Canagaratna, M. R., Zhang, Q., Worsnop, D. R., and Jimenez, J. L.: Interpretation of organic
 745 components from Positive Matrix Factorization of aerosol mass spectrometric data, *Atmos. Chem. Phys.*, 9, 2891-
 746 2918, 2009.
 747
 748 Veres, P. R., Roberts, J. M., Burling, I. R., Warneke, C., de Gouw, J., and Yokelson, R. J.: Measurements of gas-
 749 phase inorganic and organic acids from biomass fires by negative-ion proton-transfer chemical-ionization mass
 750 spectrometry (NI-PT-CIMS), *J. Geophys. Res.-Atmos.*, 115, D23302, 2010.
 751
 752 Warneke, C., Roberts, J. M., Veres, P., Gilman, J. B., Kuster, W. C., Burling, I. R., Yokelson, R. J., and de Gouw, J.
 753 A.: VOC identification and inter-comparison from laboratory biomass burning using PTR-MS and PIT-MS, *Int. J.*
 754 *Mass Spectrom.*, 303, 6-14, 2011.



755
 756 Westerling, A. L., Hidalgo, H. G., Cayan, D. R., and Swetnam, T. W.: Warming and Earlier Spring Increase
 757 Western U.S. Forest Wildfire Activity, *Science*, 313, 940-943, 2006.
 758
 759 Williams, E. J., Baumann, K., Roberts, J. M., Bertman, S. B., Norton, R. B., Fehsenfeld, F. C., Springston, S. R.,
 760 Nunnermacker, L. J., Newman, L., Olszyna, K., Meagher, J., Hartsell, B., Edgerton, E., Pearson, J. R., and Rodgers,
 761 M. O.: Intercomparison of ground-based NO_y measurement techniques, *J. Geophys. Res.-Atmospheres*, 103, 22261-
 762 22280, doi: 22210.21029/22298JD00074, 1998.
 763
 764 Wotton, B. M., Gould, J. S., McCaw, W. L., Cheney, N. P., and Taylor, S. W.: Flame temperature and residence
 765 time of fires in dry eucalypt forest, *Int. J. Wildland Fire*, 21, 270-281, 2012.
 766
 767 Yokelson, R. J., Andreae, M. O., and Akagi, S. K.: Pitfalls with the use of enhancement ratios or normalized excess
 768 mixing ratios measured in plumes to characterize pollution sources and aging, *Atmos. Meas. Tech.*, 6, 2155-2158,
 769 2013a.
 770
 771 Yokelson, R. J., Burling, I. R., Gilman, J. B., Warneke, C., Stockwell, C. E., de Gouw, J. A., Akagi, S. K., Urbanski,
 772 S. P., Veres, P., Roberts, J. M., Kuster, W. C., Reardon, J., Griffith, D. W. T., Johnson, T. J., Hosseini, S., Miller, J.
 773 W., Cocker III, D. R., Jung, H., and Weise, D. R.: Coupling field and laboratory measurements to estimate the
 774 emission factors of identified and unidentified trace gases for prescribed fires, *Atmos. Chem. Phys.*, 13, 89-116,
 775 2013b.
 776
 777 Yokelson, R. J., Crounse, J. D., DeCarlo, P. F., Karl, T., Urbanski, S., Atlas, E., Campos, T., Shinozuka, Y.,
 778 Kapustin, V., Clarke, A. D., Weinheimer, A. J., Knapp, D. J., Montzka, D. D., Holloway, J., Weibring, P., Flocke, F.
 779 M., Zheng, W., Toohey, D., Wennberg, P. O., Wiedinmyer, C., Mauldin, L., Fried, A., Richter, D., Walega, J.,
 780 Jimenez, J. L., Adachi, K., Buseck, P. R., Hall, S. R., and Shetter, R. E.: Emissions from biomass burning in the
 781 Yucatan, *Atmos. Chem. Phys.*, 9, 5785-5812, 2009.
 782
 783 Zarzana, K. J., Selimovic, V., Koss, A. R., Sekimoto, K., Coggon, M. M., Yuan, B., Dube, W. P., Yokelson, R. J.,
 784 Warneke, C., de Gouw, J. A., Roberts, J. M., and Brown, S. S.: Primary emissions of glyoxal and methylglyoxal
 785 from laboratory measurements of open biomass burning, *Atmos. Chem. Phys.*, 18, 15451-15470, 2018.
 786



Table 1. Nitrogen compounds observed in the FIREX FireLab 2016 Study.

Compound/Class	Importance	Measurement Method	References
Total Reactive N	Total available for atmospheric reactions	Catalytic Conversion NO/O ₃ chemiluminescence	Stockwell et al., 2018
Nitric Oxide	Major “flaming stage” product, oxidant production	NO/O ₃ chemiluminescence OP-FTIR	Williams et al., 1998 Selimovic et al., 2018
Nitrogen Dioxide	Atmospheric oxidant production	OP-FTIR, ACES	Stockwell et al., 2014, Min et al., 2016, Zarzana, et al., 2018
Nitrous Acid	HO _x radical source	OP-FTIR, ACES	Stockwell et al., 2014, Min et al., 2016, Zarzana et al., 2018
Nitric Acid	Particle precursor	OP-FTIR	Yokelson et al 2009, McMeeking et al 2009
Hydrogen Cyanide	Flame chemistry, Atmospheric tracer, Toxicity	OP-FTIR, PTR-ToF-MS	Selimovic, et al., 2018 Koss, et al., 2018
Isocyanic Acid	Flame chemistry, Toxicity, Health effects	PTR-ToF-MS	Koss, et al., 2018
Ammonia	Major “smoldering stage” product, Main atmospheric base, Particle formation	OP-FTIR	Selimovic, et al., 2018
NVOCs: Amides ¹ Amines ² Heterocyclics ³ Nitriles ⁴ Nitro compds ⁵	Brown carbon, Toxicity, Tracers	PTR-ToF-MS, GC/MS, I ⁻ CIMS	Koss, et al., 2018 Gilman et al., 2015 Lerner et al., 2017 Lee et al., 2014

- 1). Ethylamine, methanimine, propeneamine, sulfinylmethanamine, trimethylamine, buteneamines
- 2). Formamide, acetamide, methylmaleimide
- 3). C₂-pyrroles, dihydropyridine, ethynylpyrrole, methylpyridine, methylpyrrole, pyridinealdehyde, 4-pyridinol, vinylpyridine
- 4). Acetonitrile, acrylonitrile, benzonitrile, butanenitrile, butynenitrile, benzoacetonitrile, C₇acrylonitrile, C₈-nitriles, heptylnitrile, furancarbonitrile, methylbenzoacetonitrile, pentyl nitriles, propanenitrile, propynenitrile, butenenitrile, methylisocyanate.
- 5). Butenenitrates, nitrobenzene, nitroethane, nitroethene, nitrofurane, nitromethane, nitropropanes, nitrotoluene.



Table 2. Compounds and compound classes used in the PMF analyses and their corresponding errors.

Compound or Class	unit	Batch 1	Batch 2	Estimated error
CO ₂	ppmv	X		20% + 2 ppmv
CO	ppmv	X		20% + 0.002 ppmv
N _r	ppbv	X		10% + 1 ppbv
NH ₃	ppbv	X	X	5% + 2 ppbv
NO	ppbv	X	X	10% + 1 ppbv
NO ₂	ppbv	X	X	10% + 0.2 ppbv
HONO	ppbv	X	X	20% + 1 ppbv
HCN	ppbv	X	X	15% + 0.2 ppbv
HNCO	ppbv	X	X	15% + 0.2 ppbv
Nitriles	ppbv	X	X	20% + 0.2 ppbv
Amines	ppbv	X	X	20% + 0.2 ppbv
Amides	ppbv	X	X	20% + 0.2 ppbv
Nitro-compounds	ppbv	X	X	20% + 0.2 ppbv
Heterocyclics	ppbv	X	X	20% + 0.2 ppbv

Table 3. Summary of X_i/N_r Measurements for all Stack Burns¹

Quantity	Average ±(std dev) %
NO/N _r	34.5 (16.6)
NO ₂ /N _r	9.4 (6.2)
HNCO/N _r	6.0 (2.9)
HONO/N _r	4.5 (2.2)
HCN/N _r	4.3 (2.3)
NH ₃ /N _r	19.3 (6.7)
NVOC/N _r	4.3 (2.8)
(N _r -sumN)/N _r	15.2 (9.8)

¹). Not every measurement was available for every fire, consequently the values do not add up to exactly 100%.



Table 4. Residuals of the PMF analyses by fuel, as percent of total signal

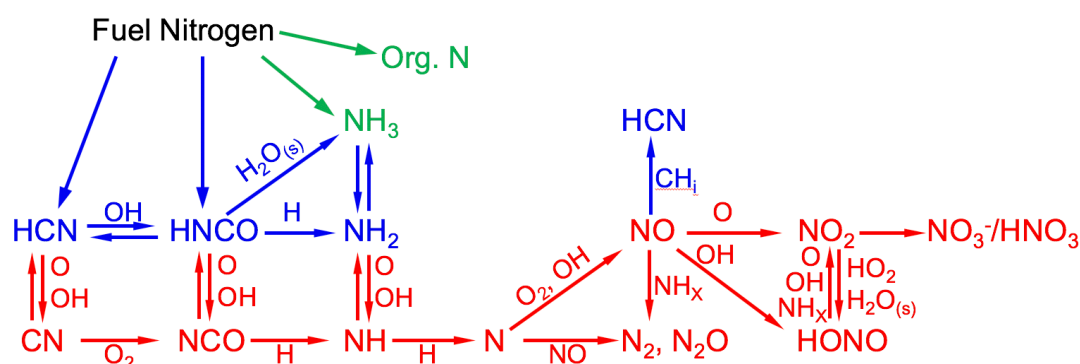
Fuel	Total Number	Component	Fire Number	Residual (%), avg (stdev)
Ponderosa Pine	9	Realistic (mix)	Fire 37,59,72	3.8 (\pm 1.4)
		Canopy (pure)	Fire 19 ^a ,39	
		Litter (pure)	Fire 38	
Lodgepole Pine	5	Realistic	Fire 07 ^a ,58,63	5.1 (\pm 3.1)
		Canopy	Fire 40	
		Litter	Fire 41	
Douglas Fir	4	Realistic	Fire 14 ^a ,57	6.8 (\pm 3.1)
		Canopy	Fire 18	
		Litter	Fire 43 ^a	
SubAlpine Fir	5	Realistic	Fire 47,67	6.6 (\pm 2.3)
		Canopy	Fire 15,23	
		Litter	Fire 51 ^a	
Engelmann Spruce	2	Realistic	Fire 08 ^a	3.1 (\pm 1.9)
		Canopy	Fire 25	
Chamise (San Dimas, CA)	2	Canopy	Fire 24,29	4.4 (\pm 2.7)
Chamise (North Mountain, CA.)	2	Canopy	Fire 27,32	4.2 (\pm 1.0)
Manzanita San Dimas, CA)	2	Canopy	Fire 30,33	4.8 (\pm 2.1)
Manzanita (North Mountain, CA.))	2	Canopy	Fire 28	5.1

^a-Excluded from Batch 2



818

819



820

821

822

823

824

825

826

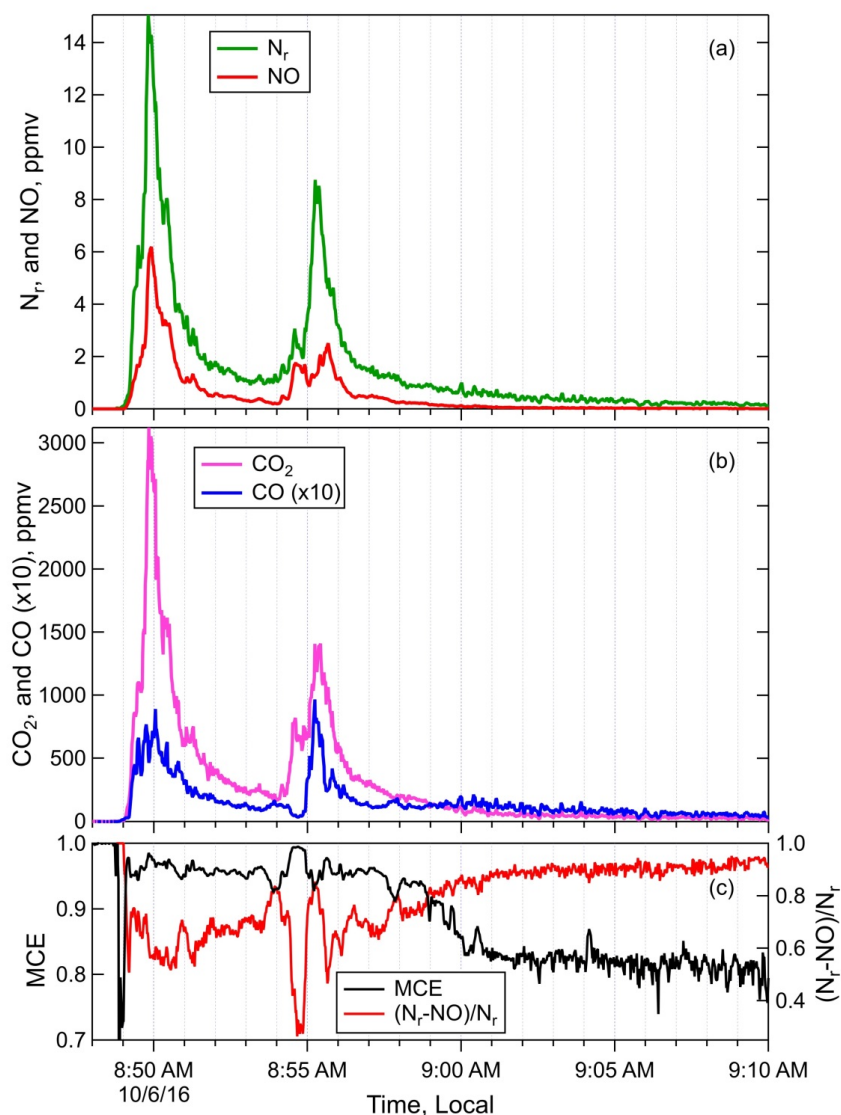
827

828

Figure 1. Schematic of the combustion chemistry of the small molecules that are emitted from BB and represent sources and sinks of reactive nitrogen (N_r), adapted from (Glarborg et al., 2018; Lobert and Warnatz, 1993; Lucassen et al., 2012). $H_2O_{(s)}$ denotes the combination of H_2O and a surface to facilitate the reaction. Red color indicates the highest temperature (combustion) processes, blue indicates intermediate temperature processes and green indicates the lowest temperature processes.



829



830

831

832 **Figure 2. Timelines of the N_r , NO (panel a), ΔCO_2 , ΔCO (panel b), MCE and $(N_r-NO)/N_r$**
 833 **(panel c) measured during Fire 004, a ponderosa pine realistic mix sample. Note that ΔCO is**
 834 **plotted at $\times 10$ the measured abundance for clarity.**

835

836

837

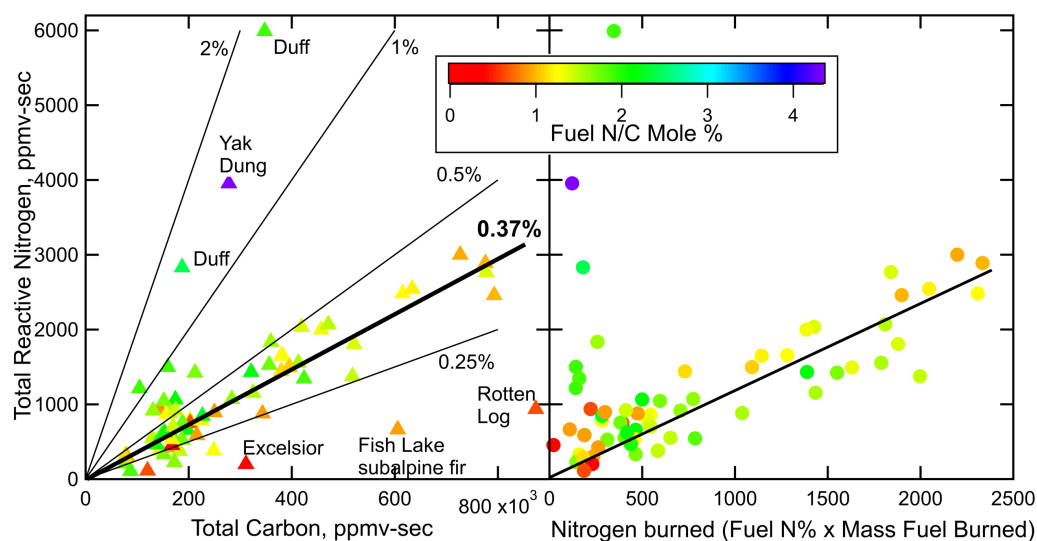
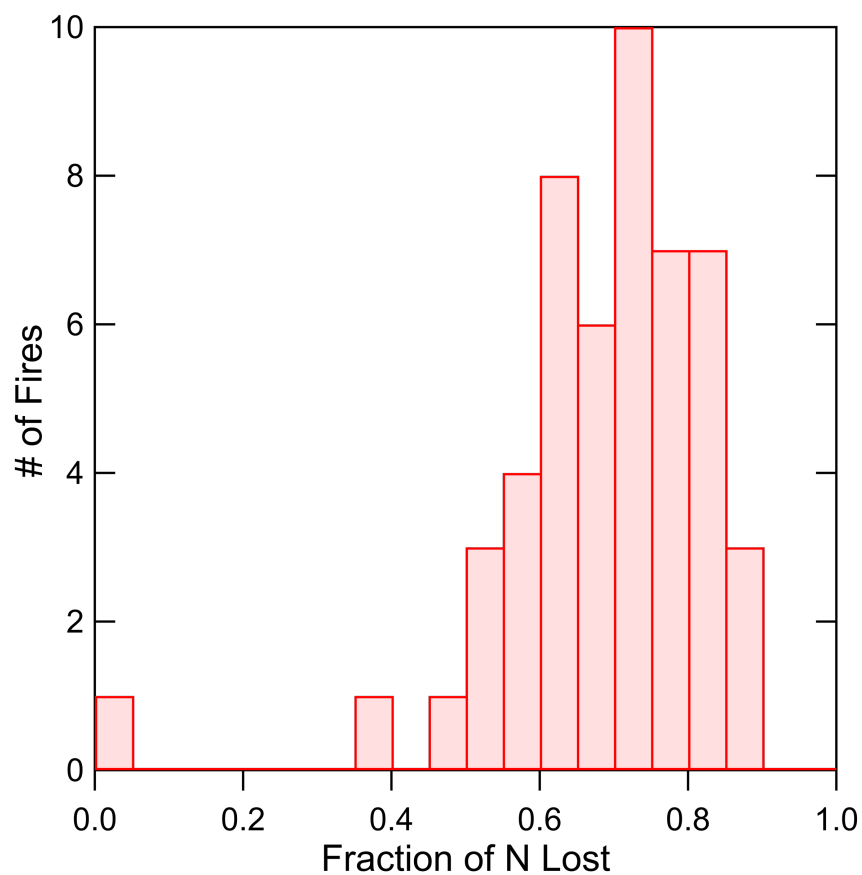


Figure 3. Integrated N_r versus integrated Total Carbon (panel a), and versus nitrogen burned based on fuel nitrogen content and mass of fuel burned (panel b). The points are colored by fuel nitrogen to carbon ratio.



845
 846

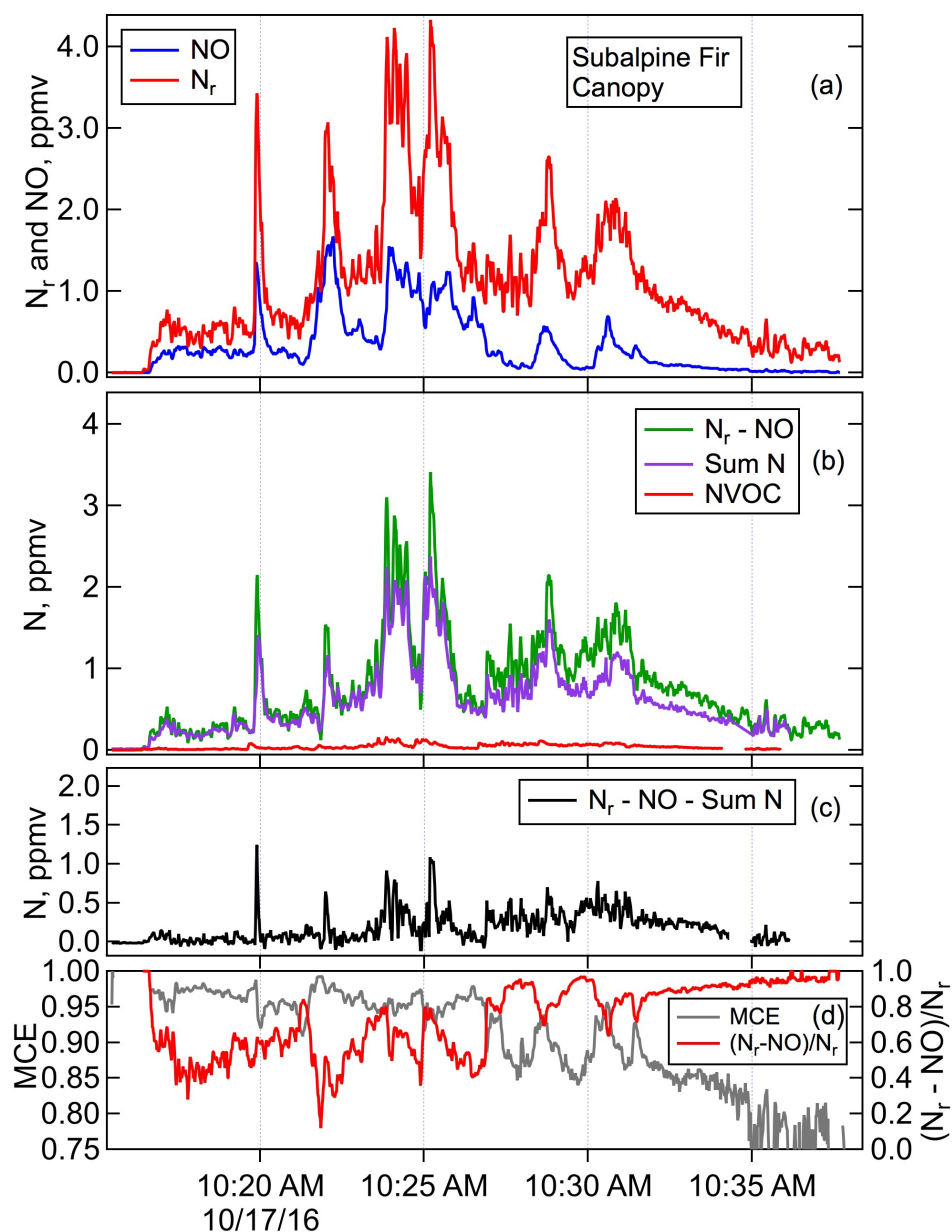


847
 848
 849
 850

Figure 4. The histogram of the fraction of N loss to N_2 and N_2O estimated from the mass balance analysis described in the Supplemental Materials (52 burns).



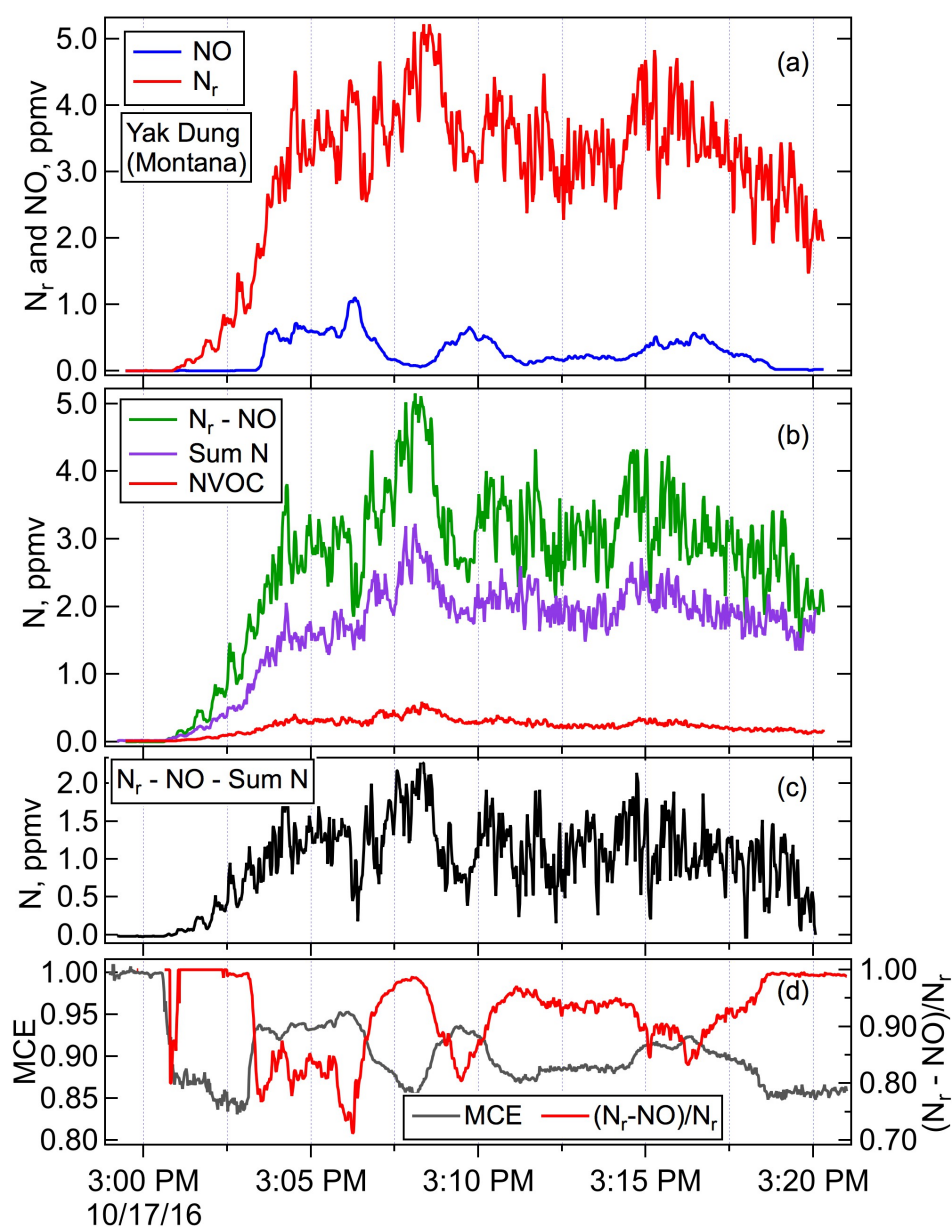
851



852
 853 **Figure 5.** Timelines of N_r and NO (panel a), $\text{N}_r - \text{NO}$, the sum of all measures N species except
 854 for NO (panel b), residual of N_r minus all measured N species ($\text{N}_r - \text{NO} - \text{Sum N}$, panel c),
 855 and MCE and $(\text{N}_r - \text{NO})/\text{N}_r$ (panel d) for Fire047, subalpine fir realistic mix.
 856



857

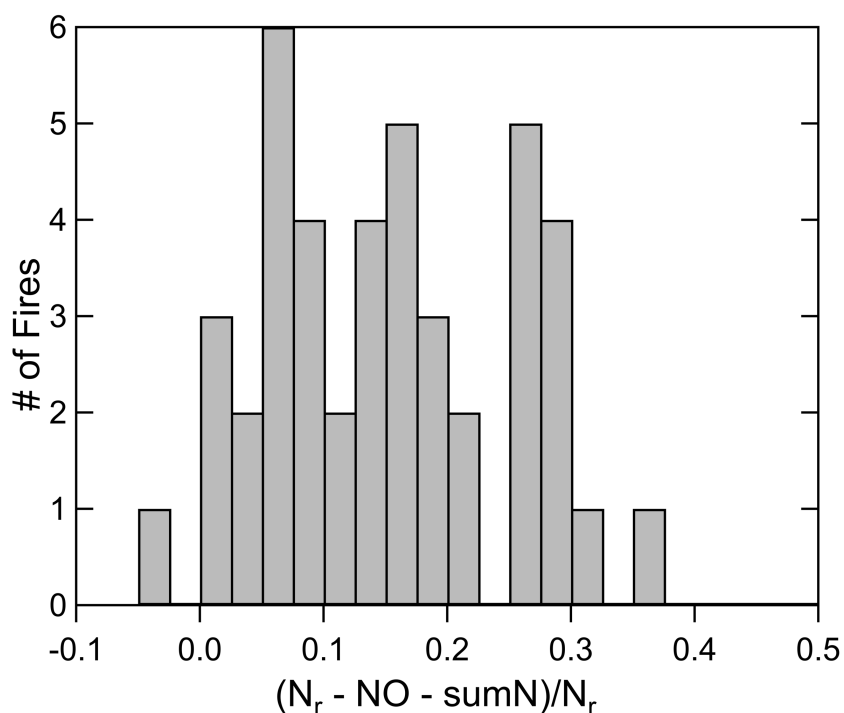


858
 859
 860
 861
 862
 863

Figure 6. Timelines of N_r and NO (panel a), N_r -NO, the sum of all measured N_r species except for NO (panel b), and residual of N_r minus all measured N species (N_r -NO-Sum N, panel c) and MCE and $(N_r$ -NO)/ N_r (panel d) for Fire050, Montana yak dung.



864
 865

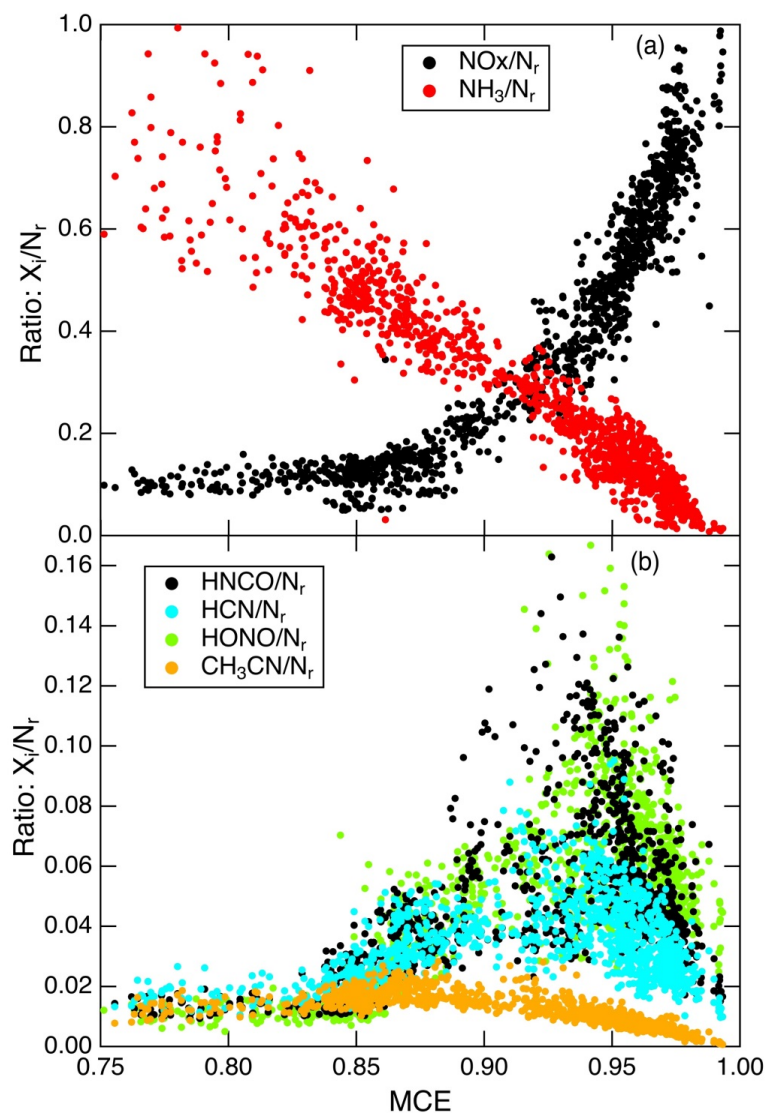


866
 867
 868
 869
 870
 871
 872

Figure 7. A histogram of the residual N for all the stack fires during the 2016 FireLab study for which there are FTIR, ACES and PTR-ToF measurements (n=43). The median is 0.143, and the mean (\pm std dev) was 0.15 (\pm 0.10).



873
 874
 875

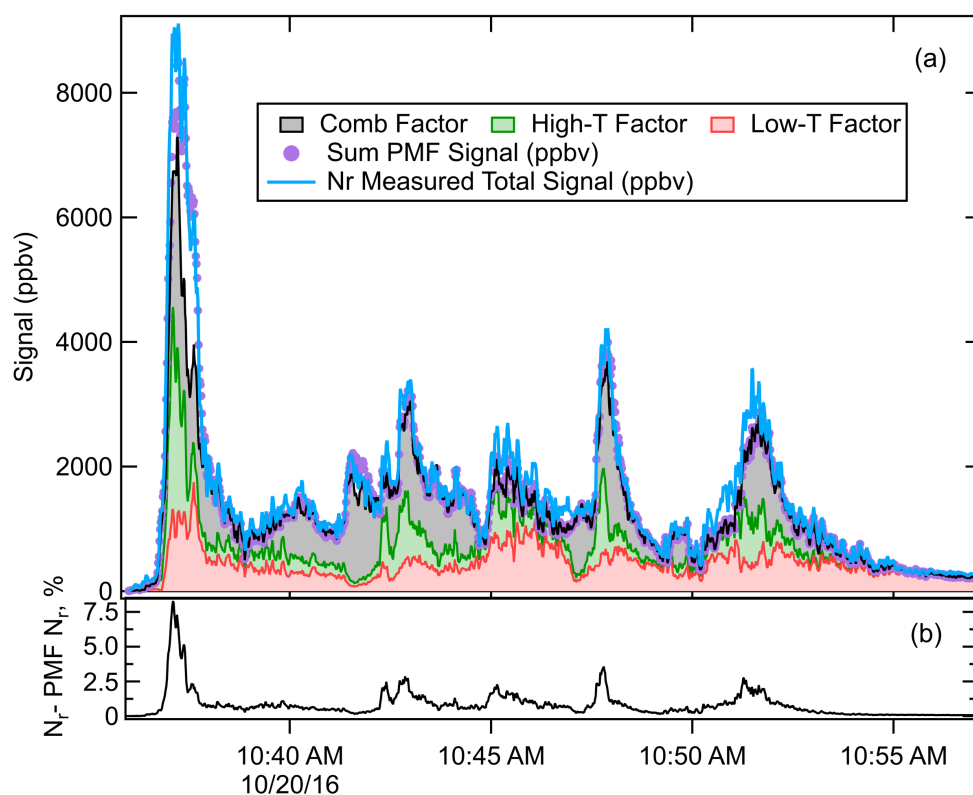


876
 877
 878
 879
 880
 881

Figure 8. The relationships between NO_x/N_r and NH_3/N_r vs MCE (panel a), and the $HNCO/N_r$, HCN/N_r , $HONO/N_r$, and CH_3CN/N_r vs MCE (panel b) for Fire 047.



882



883

884

885

886

887

888

889

Figure 9. Pane (a), the measured N_r signal for Fire 063 (lodgepole pine) (blue line), the sum of the signal reconstructed by the PMF (purple points) and the three PMF factors: combustion (grey), high temperature (green) and low temperature (red), plotted in a stacked fashion (i.e. added on top of one another). Panel (b) the “residual” of the PMF fit consisting of the measured N_r signal minus the N_r signal reconstructed by the PMF, as a percentage of the N_r signal.

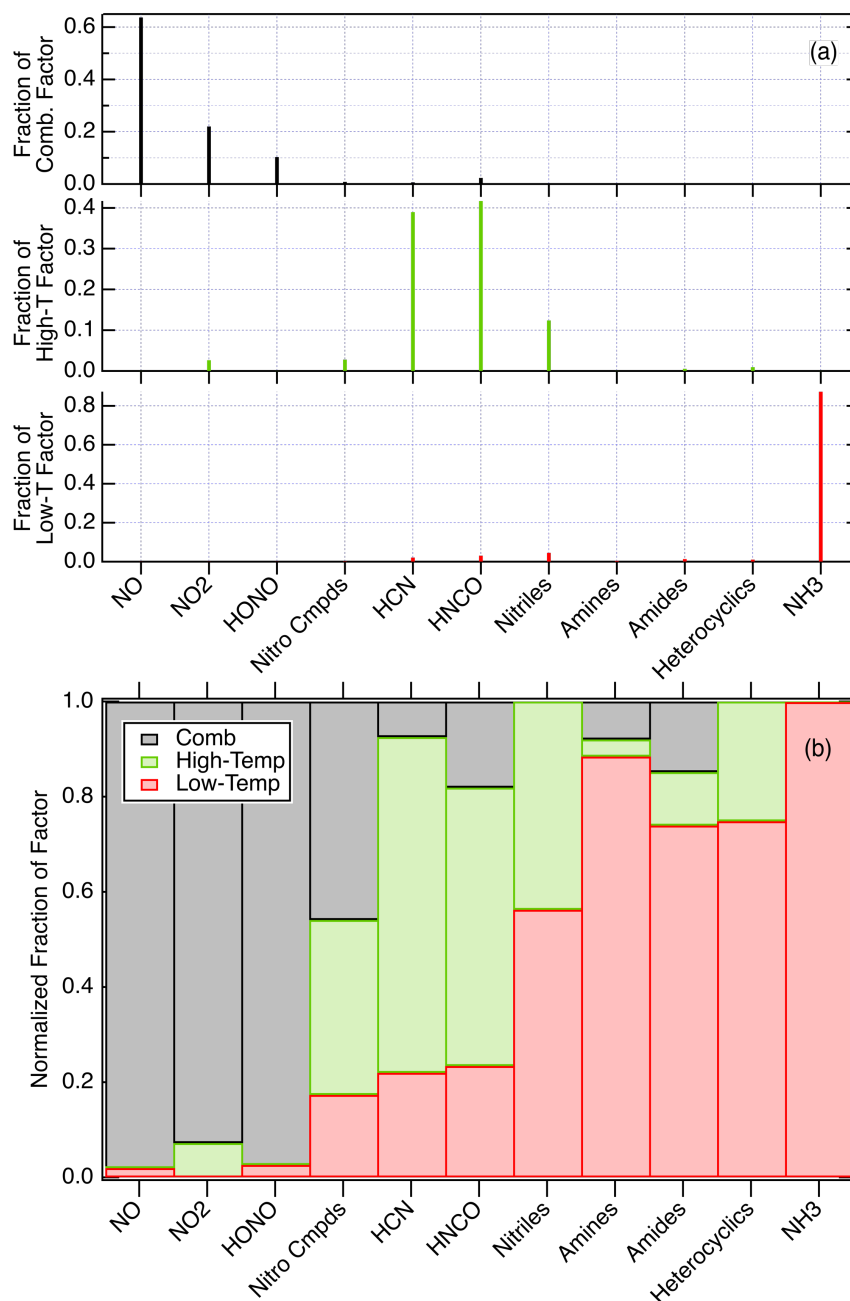


Figure 10. The contributions of nitrogen species to the factors that simulate the emissions from coniferous fuels shown in Figure S2 (panel a), and the fraction of each compound or class found in each factor (panel b).

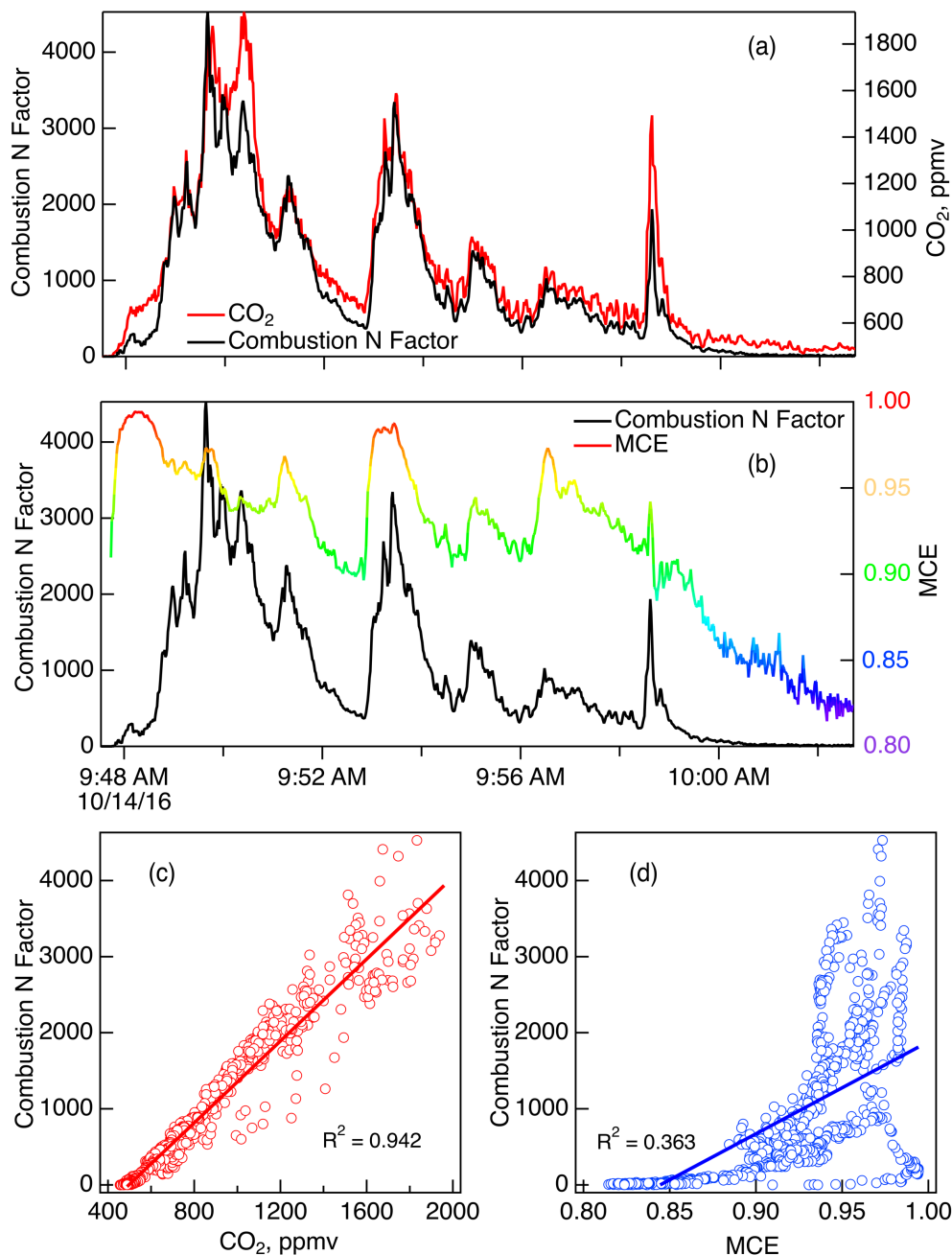


Figure 11. Comparisons of the N-PMF combustion factor (Comb-N) with CO₂ (Panel a) and MCE (Panel b) for Fire 037 (ponderosa pine). Panel (c) shows the scatter plot of the Comb-N factor versus CO₂ and panel (d) shows the scatter plot of Comb-N factor versus MCE.

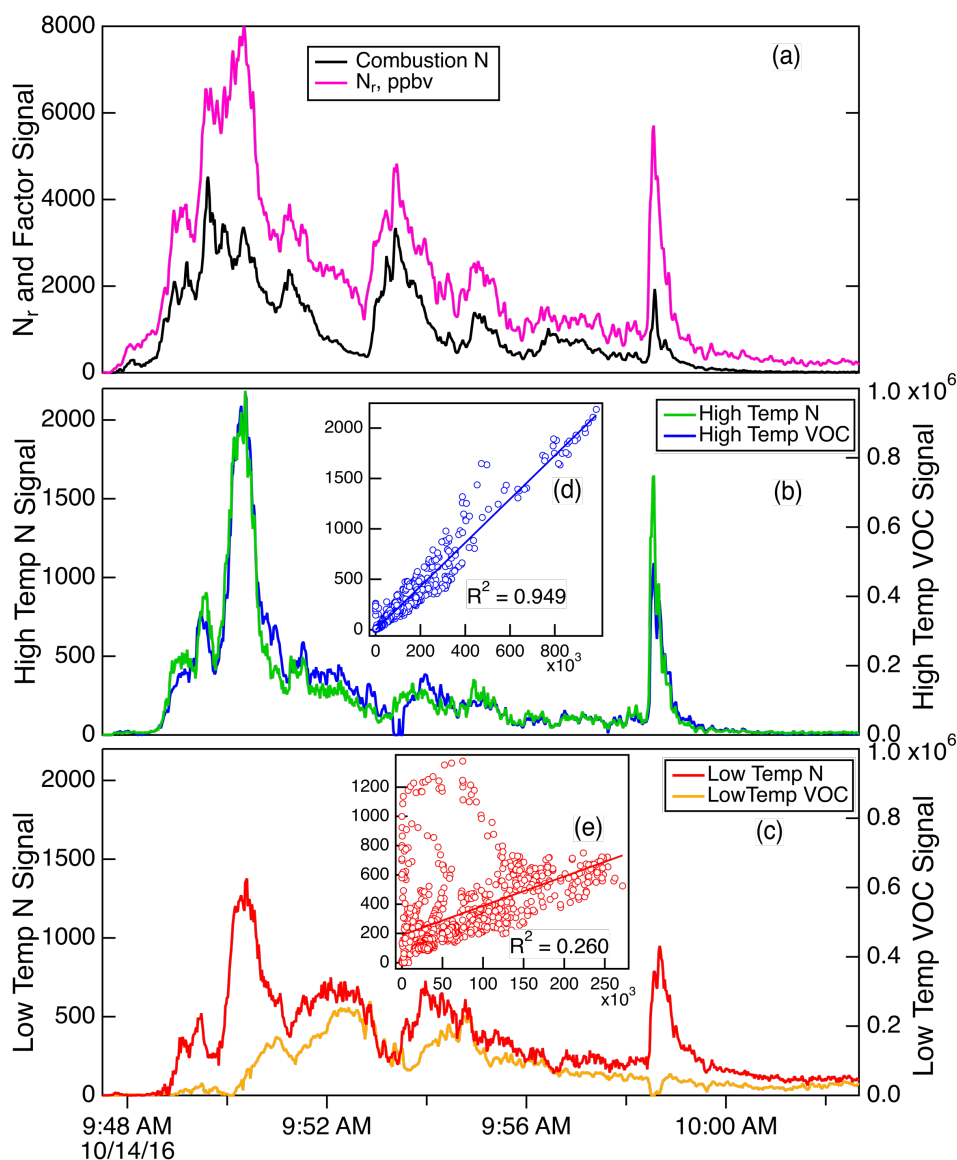


Figure 12. Details of the PMF factors for Fire 037 (ponderosa pine). Panel (a) shows the total N_r signal (magenta) and the Comb-N factor (black), panel (b) shows the HT-N factor (green) and HT-VOC factor (blue), and panel (c) shows the LT-N factor (red) and LT-VOC factor (orange). The insets (panel d) show the correlation of the two HT factors and the correlation between the two LT factors.